Molecular Biology of the Cell
Vol. 16, 2191–2206, May 2005

A *Dictyostelium* Homologue of WASP Is Required for Polarized F-Actin Assembly during Chemotaxis

Scott A. Myers,* Ji W. Han,* Yoonsung Lee,*† Richard A. Firtel,‡ and Chang Y. Chung*‡

*Department of Pharmacology, Vanderbilt University Medical Center, Nashville TN 37232-6600; and ‡Section of Cell and Developmental Biology, Division of Biological Sciences, Center for Molecular Genetics, University of California, San Diego, La Jolla, CA 92093-0634

Submitted September 27, 2004; Revised February 11, 2005; Accepted February 15, 2005
Monitoring Editor: Martin A. Schwartz

The actin cytoskeleton controls the overall structure of cells and is highly polarized in chemotaxing cells, with F-actin assembled predominantly in the anterior leading edge and to a lesser degree in the cell's posterior. Wiskott-Aldrich syndrome protein (WASP) has emerged as a central player in controlling actin polymerization. We have investigated WASP function and its regulation in chemotaxing *Dictyostelium* cells and demonstrated the specific and essential role of WASP in organizing polarized F-actin assembly in chemotaxing cells. Cells expressing very low levels of WASP show reduced F-actin levels and significant defects in polarized F-actin assembly, resulting in an inability to establish axial polarity during chemotaxis. GFP-WASP preferentially localizes at the leading edge and uropod of chemotaxing cells and the B domain of WASP is required for the localization of WASP. We demonstrated that the B domain binds to PI(4,5)P_2 and PI(3,4,5)P_3 with similar affinities. The interaction between the B domain and PI(3,4,5)P_3 plays an important role for the localization of WASP to the leading edge in chemotaxing cells. Our results suggest that the spatial and temporal control of WASP localization and activation is essential for the regulation of directional motility.

INTRODUCTION

Chemotaxis, cell movement up a chemical gradient, is central to a wide variety of biological processes in eukaryotic cells, including migration of macrophages and neutrophils during wound healing, homing of thymocytes, migration of neural crest cells, and aggregation of *Dictyostelium* cells to form a multicellular organism (Locker *et al.*, 1970; Hosaka *et al.*, 1979; Downey, 1994; Lahrtz *et al.*, 1998; Aubry and Firtel, 1999). In *Dictyostelium* cells, neutrophils, and macrophages, chemotaxis can be mediated through heterotrimeric G protein–coupled cell surface receptors. The first step of chemotactic movement is a chemoattractant-mediated increase in F-actin polymerization at the leading edge of the cell, which provides the motive force for pseudopod extension and cell movement. An important biological question is how cells regulate the formation of the leading edge in the direction of a chemoattractant source. Forward extension of the leading edge of cells is driven by the protrusion of two F-actin–rich structures, lamellipodia and filopodia. Dissecting the signaling mechanisms controlling F-actin organization is a key step toward understanding directed cell movement.

The WASP (Wiskott-Aldrich Syndrome protein) family has emerged as important regulatory molecules that connect multiple signaling pathways through Rac/Cdc42 to F-actin polymerization. In mammals, this family includes WASP, N-WASP, and SCAR or WAVE (Miki *et al.*, 1996; Bear *et al.*, 1998). The expression of WASP appears to be restricted to hematopoietic cells (Ochs, 1998b), whereas the closely related N-WASP is more widely expressed (Miki *et al.*, 1996). Wiskott-Aldrich Syndrome (WAS) is a human X-linked immunodeficiency characterized by recurrent infections, hematopoietic malignancies, eczema, and thrombocytopenia that is caused by mutations in the gene encoding WASP (Aldrich *et al.*, 1954; Derry *et al.*, 1994; Snapper *et al.*, 1998). The size of hematopoietic cells, including platelets, neutrophils, and lymphocytes, is significantly reduced in WAS patients, and the cell surfaces are relatively smooth with a decrease in the number and size of microvilli, suggesting a defect in cytoskeletal architecture (Remold-O'Donnell *et al.*, 1997). Chemotaxis of macrophages and monocytes from WAS patients is significantly defective.

WASP and N-WASP are complex "adaptor" proteins thought to link multiple signaling inputs to regulate the actin cytoskeleton. Both WASP and N-WASP possess a WH1 (WASP homology 1) domain, a basic (B) domain, a Cdc42/Rac binding (GBD) domain, a polyproline (SH3-binding) domain, a G-actin–binding verprolin homology (V) domain (sometimes referred as WH2 domain), a central domain (C), and a C-terminal acidic (A) segment (Symons *et al.*, 1996; Zigmond, 2000). The GBD domain of WASP interacts with the GTP-bound form of Cdc42 and Rac (Symons *et al.*, 1996), key regulators of the actin cytoskeleton (Hall, 1998). SCAR/WAVE family proteins possess a C-terminal VCA domain similar to WASP and N-WASP, but have a long N-terminal domain lacking the WH1 and GBD domains (Miki *et al.*, 1996; Bear *et al.*, 1998; Marchand *et al.*, 2001). WASP, N-WASP, and SCAR/WAVE have been shown to activate the Arp2/3 complex, via C-terminal A segment, to stimulate

This article was published online ahead of print in *MBC in Press* (http://www.molbiolcell.org/cgi/doi/10.1091/mbc.E04–09–0844) on February 23, 2005.

† Present address: Department of Cell Biology, Duke University Medical Center, Durham, NC 27710.

Address correspondence to: Chang Y. Chung (chang.chung@vanderbilt.edu).

actin polymerization (Machesky and Insall, 1998; Machesky *et al.*, 1999; Rohatgi *et al.*, 1999). Biochemical and structural data suggests that WASP is held in an inactive configuration through the binding of an autoinhibitory domain that overlaps with the GBD to the C region of the VCA domain (Prehoda *et al.*, 2000). WASP is activated by signaling pathways through the binding of Rac/Cdc42-GTP to the GBD, resulting in a conformational change, which allows the VCA domain to activate the Arp2/3 complex (Kim *et al.*, 2000). The presence of a GBD domain and the interaction between WASP and Arp2/3 suggest that signaling pathways may regulate the spatial and temporal control of WASP function, in part, through receptor activation of Cdc42/Rac leading to actin cytoskeleton reorganization. Previous studies have suggested WASP changes its conformation from auto-inhibited to active upon binding of activated Cdc42 ($Cdc42^{GTP}$) and other ligands, such as $PI(4,5)P_2$ (Higgs and Pollard, 2000; Rohatgi *et al.*, 2000).

However, in order to better understand WASP function, we require a dynamic in vivo system in which spatial and temporal regulation of WASP function in a biological response can be dissected. In vivo studies suggest that WASP is involved in controlling directional motility during chemotaxis and the spatial organization of F-actin in T-cell activation. Chemotaxis of macrophages from WAS patients is significantly impaired, whereas the speed of random motility of both cell types was found to be indistinguishable from that of control cells (Altman *et al.*, 1974; Ochs, 1998a; Zicha *et al.*, 1998). Monocytes from WAS patients do not effectively polarize and also have severely impaired migration in response to a variety of chemotactic agents (Badolato *et al.*, 1998; Zicha *et al.*, 1998). To better understand the role WASP in directional movement, we have examined spatial and temporal regulation of WASP function in *Dictyostelium*. Through the analysis of WASP mutants, we demonstrated that WASP is required for cellular polarity and motility during chemotaxis of *Dictyostelium*. We demonstrated that WASP localization can be differentially regulated by the interaction of the B domain with $PI(4,5)P_2$ and $PI(3,4,5)P_3$. Further, we provide evidence that WASP localization to the leading edge requires the basic domain interacting with $PI(3,4,5)P_3$, the product of PI3Kinase. We suggest that the spatial and temporal control of WASP localization and activation is essential for the regulation of directional motility.

MATERIALS AND METHODS

Cell Culture and Development

Dictyostelium cells were cultured axenically in HL5 medium supplemented with 60 U of penicillin and 60 μg of streptomycin per ml. For examining developmental phenotypes, cells were washed twice with 12 mM Na/K Phosphate buffer and plated on nonnutrient agar plates.

Molecular Biology

Dictyostelium WASP was originally identified in a two-hybrid screen with constitutively active human Cdc42 as a bait. The screening was essentially done as previously described (Chung *et al.*, 1998). A cDNA containing a 1200-base pair open reading frame (ORF) for WASP was isolated. The plasmid for homologous recombination was constructed by insertion of Bsr gene cassette into the WASP ORF at the *Bam*HI site or THY1 gene at the *Eco*RI site of WASP genomic DNA. The Bsr targeting construct was linearized with *Sac*I and *Xho*I and electroporated into Ax2 wild-type cells, and transformants were selected and screened for disruption of WASP by Southern blot analysis ($WASP^{hypo}$ strain). The THY targeting construct was linearized with *Bgl*II/*Xho*I and electroporated into the thymidine auxotrophic strain, JH10, and transformants were selected in the absence of thymidine in the medium and screened for disruption of WASP. Southern blot analysis showed this strain of cells ($WASP^{THY}$) still has a copy of WASP gene not disrupted and this strain was used to create a knock-in strain.

We used a knock-in approach to acquire a strain that has very low level of WASP expression. The targeting construct was made by cloning 500 base pairs of WASP genomic DNA encompassing the start codon in *Spe*I-*Hin*dIII site of pBSSK(+). A Bsr gene cassette was cloned into *Bam*HI site and WASP cDNA fused with YFP at the N-terminus under the control of a tetracycline-responsive element (TRE) was cloned into *Eco*RI-*Xho*I. TRE is the binding site for a chimeric tetracycline-controlled transcriptional activator protein (tTA). In the absence of tetracycline, tTA binds to its target sequence and strongly induces gene expression. Tetracycline prevents tTA from binding to the tetracycline-responsive element, rendering the promoter virtually silent, enabling us to get a strain expressing a very low level of WASP. The targeting vector was cut with *Spe*I-*Xho*I and transformed into $WASP^{THY}$ cells, and positive clones were selected in the presence of blasiticidine and identified by Southern blot. By homologous recombination, the knock-in construct replaced the WASP gene with a WASP allele under TRE regulation. By differing the concentration of tetracycline in the medium, we were able to elucidate defects in actin polymerization and chemotactic motility in different levels of WASP expression. Cells were transformed with a vector encoding RNA complementary to WASP mRNA under the control of the *discoidin* promoter that can be negatively regulated by folic acid and turned on by starvation. The GFP-WASP vector was constructed by cloning the sequence encoding eGFP in-frame with the entire coding sequence of WASP that was amplified by PCR. The construct encoded fusion proteins with GFP at the N-terminus, separated by the flexible linker GSGSG from the entire coding sequence of WASP. The GFP fusion proteins were expressed under control of the actin-15 promoter using the pEXP4(+) vector.

In Vivo Actin Polymerization Assay

F-actin was quantified from TRITC-phalloidin staining of *Dictyostelium* cells as described in the previous study (Zigmond *et al.*, 1997). Cells were pulsed with 30 nM cAMP at 6-min intervals for 5 h. Cells were diluted to 1×10^7 cells/ml and shaken at 200 rpm with 2 mM caffeine for 20 min to synchronize the signaling of the cells. Cells were spun and resuspended with phosphate buffer (10 mM PO_4 buffer, pH 6.1, and 2 mM $MgSO_4$) at 5×10^7 cells/ml and stimulated with 100 μM cAMP. Five hundred microliters of cells were taken at 5, 10, 20, 30, 50, and 80 s time points and mixed with actin buffer (20 mM KH_2PO_4, 10 mM PIPES, pH 6.8, 5 mM EGTA, 2 mM $MgCl_2$) containing 6% formaldehyde, 0.15% Triton X-100, and 1 μM TRITC phalloidin. Cells were fixed and stained for 1 h and spun down at 14,000 rpm for 5 min in the microfuge. Pelleted cells were extracted with 1 ml of 100% methanol, and fluorescence was measured (540ex/575em). To determine nonsaturable binding, 100 μM unlabeled phalloidin was included.

F-actin Staining

For phalloidin staining, cells were starved in 12 mM sodium phosphate buffer (pH 6.2) for more than 5 h and fixed with 3.7% formaldehyde for 5 min. Cells were permeabilized with 0.5% Triton X-100, washed, and incubated with FITC- or TRITC-labeled phalloidin (Sigma, St. Louis, MO) in phosphate-buffered saline (PBS) containing 0.5% bovine serum albumin (BSA) and 0.05% Tween-20 for 1 h. Cells were washed in PBS containing 0.5% Tween-20. Images were captured with Roper Coolsnap camera (Tucson, AZ) and Metamorph software (Universal Imaging, West Chester, PA).

For labeling barbed-ends, aggregation competent cells were permeabilized with 100 mM PIPES, pH 6.9, 1% Triton X-100, 4% PEG, 1 mM EGTA, 1 mM $MgCl_2$, 3 μM phalloidin for 3 min, and 0.4 μM Rhodamine-labeled actin in 1 μM ATP solution was added. After 5 min staining, cells were washed three times with PIPES buffer and fixed with 3.7% paraformaldehyde.

Chemotaxis Assay

Cells competent to chemotax toward cAMP (aggregation-competent cells) were obtained by pulsing cells in suspension for 5 h with 30 nM cAMP, conditions that maximally induce the expression of aggregation-stage genes required for aggregation, including the cAMP receptor cAR1 and the coupled G protein α subunit Gα2. The chemotaxis assays were done as previously described (Chung and Firtel, 1999; Meili *et al.*, 1999). Cells were pulsed with 30 nM cAMP at 6-min intervals for 5 h and plated on glass-bottomed microwell dishes (MarTek, Ashland, MA). A micropipette filled with 100 μM cAMP was positioned to stimulate cells by using a micromanipulator (Eppendorf, Hamburg, Germany) and the response and movement of cells were recorded by using Metamorph software (1 image per every 6 s). Cell movement was examined by tracing the movement of a single cell in a stack of images.

Lipid-binding Assay

PIP strips (Echelon, Salt Lake City, UT) were blocked with 3% (wt/vol) fatty acid–free BSA in TBST (10 mM Tris-HCl, pH 8.0, 150 mM NaCl and 0.1% [vol/vol] Tween-20) for 1 h. Blocked membranes were incubated for 2 h at 4°C with 100 ng/ml GST fusion protein and then washed five times for 5 min each with TBST. After washing, membranes were incubated with anti-GST monoclonal antibody for 1 h (Santa Cruz Biotechnology, Santa Cruz, CA), followed by additional washing and incubation with an anti-mouse horseradish-peroxidase conjugate (Amersham, Piscataway, NJ). After final washing, chemi-

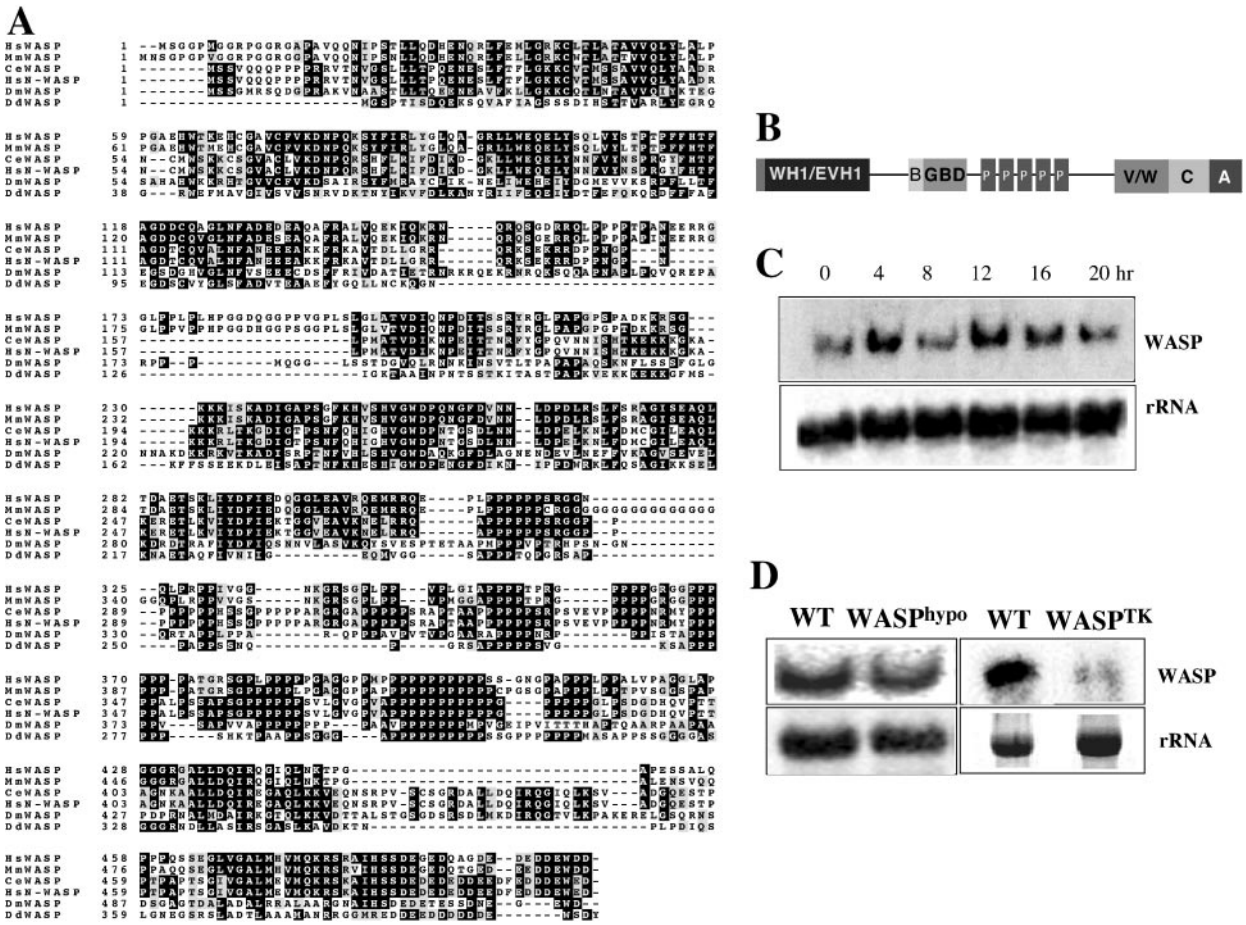

Figure 1. Deduced sequence of *Dictyostelium* WASP. (A) Sequence comparison of *Dictyostelium* WASP with WASPs from other species. Deduced amino acid sequence of WASP from the 1200-base pair DNA clone is aligned with human (Hs), mouse (Mm), *Caenorhabditis elegans* (Ce), and *Drosophila* (Dm) WASP. (B) Schematic diagram of WASP domain structure. WH1, WASP homology I domain; B, Basic domain; GBD, Cdc42/Rac binding domain; V, Verprolin homology domain; C, central domain; A, acidic domain. (C) Northern blot showing the developmental time course of WASP expression. Total RNA of 16 μg/sample was resolved on a 1.0% denaturing agarose gel, blotted, and probed as described previously (Datta and Firtel, 1987). The 0-h time point is for vegetative cells. (D) Northern blot showing reduction of WASP transcript in WASP^{hypo} cells and the lack of WASP transcript in WASP^{TK} cells.

luminescence was then used to detect binding of GST fusions to phospholipids. Densitometry was conducted using NIH Image.

PIP beads (Echelon) were washed twice with 5 volumes of wash/binding buffer (20 mM Tris, pH 7.4, 150 mM NaCl, 0.05% Tween 20, 1% ovalbumin) for 1 h. Control beads without cross-linked lipid were prepared in an identical manner. GST-B-GBD protein (5 μg) was then added to the tubes, and the protein was allowed to bind for 2 h at 4°C with gentle agitation. The tubes were then centrifuged briefly, the beads were washed two times with 0.5 ml of wash/binding buffer, and the bound proteins were eluted by boiling the beads in 20 μl of Laemmli sample buffer containing 5% 2-mercaptoethanol. The proteins were then separated on a 10% SDS-PAGE gel. GST-B-GBD protein was detected by Western blot.

Liposomes were prepared using phosphatidylcholine (PC; Sigma) or synthetic PC phosphatidylcholine (Avanti Polar Lipids, Birmingham, AL) and 5% of the phospholipid of interest (150 μg of total phospholipid). Phospholipids were resuspended in chloroform, mixed, and dried down in glass tubes under nitrogen. The lipid film was resuspended in resuspension buffer (50 mM HEPES, KOH [pH 7.6], 100 mM KCl, 1 mM EGTA, and 1 mM dithiothreitol) at a final concentration of 1 μg/μl, vortexed vigorously for 5 min, and then placed in a bath sonicator for 5 min at 4°C. To perform binding assay, 25 μg of GST-YFP-BG or GST proteins, 50 μg of the appropriate liposomes, 50 μl of 2% ovalbumin (Sigma), and 10 μl of protease inhibitor cocktail (Sigma) were mixed in binding buffer (0.25 M sucrose, 1 mM EDTA, and 20 mM Tricine, pH 7.8). Immediately after incubation, GST fusion protein and liposome complex were overlaid on an Optiprep (Greiner BioOne, Longwood, FL) step gradient (5 ml of 40%:2 ml of 30%:1.6 ml of 15%:1.6 ml of 5% of Optiprep in binding buffer) and centrifuged in a Beckman SW40Ti rotor (Fullerton, CA) for 18 h at 35,000 rpm at 4°C. Five hundred-microliter fractions were collected from the top of tubes and analyzed by SDS-PAGE, followed by either immunoblot with anti-GST polyclonal antibody (Santa Cruz Biotechnology) or Coomassie-stained analysis. Protein bands were quantified using NIH image software (NIH).

RESULTS

Dictyostelium WASP

Dictyostelium WASP was identified by yeast two-hybrid screen with constitutively active HsCdc42 as bait as described in the previous study (Chung *et al.*, 1998). The WASP ORF encodes a protein of 399 amino acids (Figure 1A; GenBank accession no. AAG24442; locus name: *wasA*). Direct pair-wise comparison with human WASP indicates that two proteins are 32% identical and 44% similar. Multiple sequence alignments with WASP from other species indicates that WASP has similar domain architecture, as depicted in Figure 1B, to that of mammalian WASP. Northern blot analysis shows that WASP expression is developmentally regulated with peaks of expression during aggregation and multicellular stages, suggesting a role for cellular motility during aggregation and morphogenesis in the multicellular stages of development (Figure 1C).

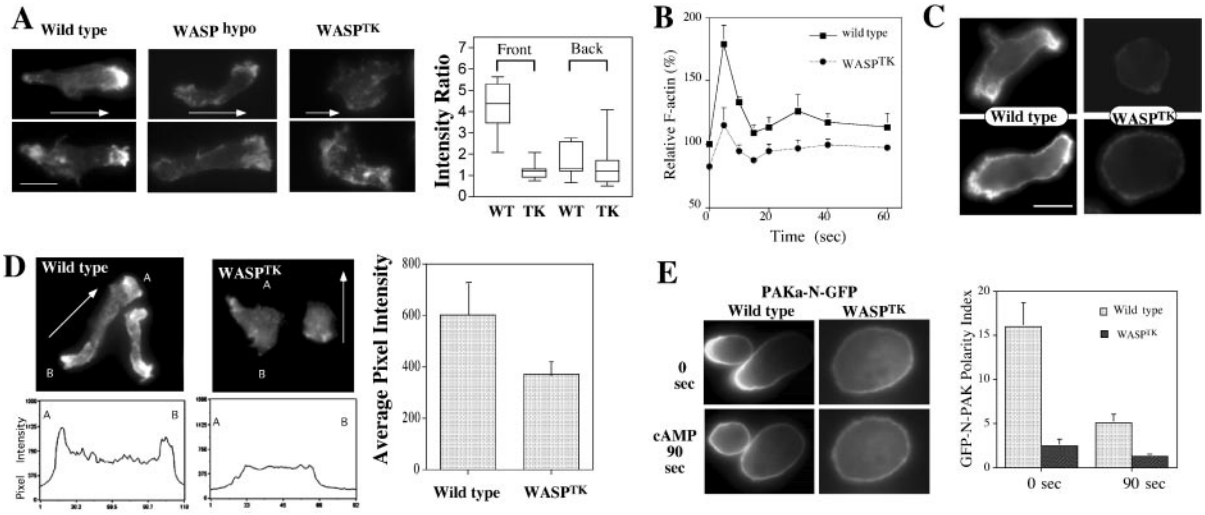

Figure 2. F-actin organization of cells expressing low levels of WASP. (A) F-actin organization revealed by phalloidin staining in WASP^{hypo} and WASP^{TK} cells under cAMP gradient. Stainings of two cells with representative phenotypes are shown. Arrows indicate the direction of cAMP gradient. Right panel shows ratio of intensity of F-actin staining at the foremost part (front) or rear end (back) of cells divided by the intensity of the center of cells. Intensity value was acquired by linescan of images in the direction of the gradient (n = 10). (B) In vivo actin polymerization assay measuring F-actin assembled in response to the chemoattractant (cAMP) stimulation. Note that F-actin polymerization upon cAMP stimulation is defective in WASP^{TK} cells. (C) F-actin organization revealed with ABP-GFP in live cells. ABP-GFP fusion protein binds specifically and dynamically to the same F-actin structures that phalloidin recognizes in fixed cells. (D) Distribution of free barbed end in cells. Rhodamine-labeled actin (0.4 μM) was incorporated into permeabilized cells to visualize free barbed-ends for actin polymerization in wild-type cells or WASP^{TK} cells. Linescans of a cell from point A to B were shown in bottom panels. Incorporation of Rhodamine-labeled G-actin was quantified by measuring the fluorescence intensity and shown in right panel (n = 6). (E) Axial polarity of wild-type and WASP^{TK} cells. GFP fusion of N-terminal half of PAKa (PAKa-N-GFP) shows specific localization to uropod of polarized cells and was used as a reporter to examine cellular polarity. Aggregation competent wild-type cells are well polarized and showed biased localization of PAKa-N-GFP at the uropod, but WASP^{TK} cells show almost equal distribution of PAKa-N-GFP, indicating lack of axial polarity. Polarity index was calculated by the ratio of PAKa-N-GFP intensity at the leading edge to GFP intensity at the uropod and shown in the right panel (n = 6). The polarity index of wild-type cells is significantly greater than that of WASP^{TK} cells.

WASP Deletion Mutants

Southern blot analysis revealed two copies of genes encoding WASP in the *Dictyostelium* genome (unpublished data). To investigate WASP function, we attempted to generate a *wasp* null mutant. We have not been able to obtain a null mutant (knockout of both copies of the gene) using standard homologous recombination approaches, possibly because such a strain may exhibit severe growth defects and thus be selected against using the standard protocol. The level of WASP expression in cells stably expressing WASP antisense RNA is normally 20–40% of that of wild-type cells and we have been unable to obtain stable antisense cell lines exhibiting less WASP mRNA expression (unpublished data). However, we were able to disrupt one of the copies of the WASP gene by homologous recombination, and analysis of this hypomorphic strain (WASP^{hypo}) has provided us with direct evidence for involvement of WASP in the in vivo regulation of F-actin assembly and cell motility during chemotaxis (see below). To acquire a strain that has a very low level of WASP expression, we made a knockin construct in which the level of WASP expression is regulated transcriptionally by a tetracycline (Tet)-regulated promoter/transcription activator combination (Tet-Off TA; tTA; Blaauw *et al.*, 2000; Funamoto *et al.*, 2002). This construct was used to create a knock-in strain by replacing intact WASP gene with WASP under the control of tTA in the single WASP gene null background (WASP^{THY} starin). WASP knockin cells (WASP^{TK}) express a very low level of WASP transcript in the absence of the Tet-off TA transcription activator (Figure 1D).

Aberrant F-actin Organization and Loss of Polarity in Cells Expressing Low Levels of WASP

To examine whether reduced expression of WASP has an impact on the actin cytoskeleton, we stained for actin filaments of aggregation-competent WASP^{hypo} cells under the cAMP gradient using rhodamine-phalloidin staining. The actin cytoskeleton controls the overall structure of cells and is highly polarized in chemotaxing cells, with F-actin localized predominantly in the anterior leading edge and to a lesser degree in the cell's posterior (Gerisch *et al.*, 1995; Westphal *et al.*, 1997; Parent and Devreotes, 1999; Firtel and Chung, 2000). Wild-type cells are well polarized and show localized F-actin assembly at lamellipodia of the leading edge and, to a lesser degree, at the posterior cortical region of the retracting cell body (uropod; Figure 2A). WASP^{hypo} cells appear elongated and polarized but show significantly less F-actin at the leading edge. Moreover, F-actin at the uropod is almost not detectable. WASP^{TK} cells exhibited even stronger defects in F-actin organization. These cells exhibit neither a prominent F-actin–enriched lamellipod nor cell polarity and were not elongated, presumably because of the lack of polarized organization of F-actin. Some of WASP^{TK} cells seem to maintain lower but polarized distribution of F-actin. To determine if this polarized distribution is in the direction of cAMP gradient, we measured fluorescence intensity by performing linescan of images in the direction of the gradient and determined ratio of intensity of F-actin staining at the foremost part (front) or rear end (back) of cells divided by the intensity of the center of cells. Wild-type cells showed five times higher F-actin staining at

front, whereas WASP^{TK} cells showed virtually the same intensity of the center of cell, indicating the polarized distribution of F-actin, if any, is not in the direction of cAMP gradient.

WASP^{TK} cells were tested for in vivo actin polymerization responses to cAMP stimulation. Wild-type cells show a rapid and transient increase of F-actin assembly (~70–90% increase) by 10 s after cAMP stimulation (Figure 2B), as previously described (Zigmond *et al.,* 1997). WASP^{TK} cells have a moderately lower level of F-actin assembly in unstimulated cells. On chemoattractant stimulation, these cells show a significantly reduced level of actin assembly, which is presumably due to the lower expression of WASP.

To investigate spatial regulation of F-actin organization in living cells, we used the green fluorescent protein–actin-binding domain (GFP-ABD) probe (Pang *et al.,* 1998) that is a fusion of EGFP and the actin-binding domain from ABP-120, the major F-actin cross-linking protein in *Dictyostelium* cells (Bresnick *et al.,* 1990). The fusion protein binds specifically and dynamically to the same F-actin structures that phalloidin recognizes in fixed cells. In chemotaxing wild-type cells, prominent accumulation of GFP-ABD was observed at the leading edge and uropod (Figure 2C). In addition, there was a moderate localization of GFP-ABD along the entire cell cortex. However, in WASP^{TK} cells, GFP-ABD is more diffusely distributed, and no polar distribution is observed, consistent with the results of the phalloidin staining shown in Figure 2A. More importantly, as shown in Figure 2D, WASP^{TK} cells show a greatly decreased number of free barbed ends relative to wild-type cells, as might be expected because of the lack of WASP. In aggregation-competent wild-type cells, the distribution of free barbed ends was very polarized. In WASP^{TK} cells, the labeling of free barbed ends is greatly reduced and is not localized. This observation is consistent with our findings in phalloidin staining and in agreement with models suggesting that WASP is required for polarized F-actin assembly in migrating cells.

Localized myosin II assembly is key in maintaining cell polarity and cortical tension and retracting the posterior cell body (Egelhoff *et al.,* 1996; Stites *et al.,* 1998; Clow and McNally, 1999; Sanchez-Madrid and del Pozo, 1999;). PAKa plays important roles for the regulation of cell polarity, chemotaxis, and cytokinesis in *Dictyostelium* by controlling myosin II assembly (Chung and Firtel, 1999). Our previous study demonstrated that the N-terminal domain of PAKa is necessary and sufficient for PAKa's localization to the posterior cortex of polarized, chemotaxing cells (Chung and Firtel, 1999; Chung *et al.,* 2001). We used a GFP fusion of N-PAKa (N-PAKa-GFP) as a reporter to examine axial polarity of cytoskeleton. Wild-type cells showed biased distribution of N-PAKa-GFP at the uropod in chemotaxing cells, as expected (Figure 2E). When this polarity is disrupted by globally stimulating cells (bathing the cells in cAMP to simultaneously activate all of the cell-surface cAMP receptors), N-PAKa-GFP becomes uniformly distributed around the cells' periphery. As the rounded morphology of WASP^{TK} might predict, N-PAKa-GFP is distributed more uniformly along the cortex of these cells compared with wild-type cells, indicating that establishment of cytoskeleton polarity is significantly impaired in WASP^{TK} cells.

Chemotaxis of WASP Mutants

To test whether the changes in the actin cytoskeleton described above alter chemoattractant-induced cell migration, we used a chemotaxis assay combined with time-lapse video microscopy (Figure 3). Wild-type cells are usually well polarized, move quickly and linearly toward the cAMP source, extend pseudopodia predominantly in the direction of cAMP gradient, and produce very few random lateral or rear pseudopodia. Cells of WASP^{hypo} strain exhibit less vigorous pseudopodia extension and do not appear to retract the uropod as efficiently as wild-type cells (Figure 3A). Pseudopod extension and uropod retraction of wild-type cells are well coordinated so that the length of cell body of migrating cells is relatively constant (Figure 3C). WASP^{hypo} cells appear defective in this process, which is consistent with their lack of F-actin assembly at the uropod (Figure 2A). The rear cell body of the WASP^{hypo} cells does not retract actively, whereas pseudopod extension is not largely impaired. This results in a very elongated cell body and greater variations in cell body length as depicted in Figure 3B. Mechanical tension caused by extension of pseudopod forced the posterior of WASP^{hypo} cells to become detached from the substratum and contracts, resulting in abrupt shortening of the length of cell body (Figure 3C). WASP^{TK} cells have even greater defects in chemotaxis. They are very flattened and round as they are unable to establish polarity (Figure 3A). Some of WASP^{TK} cells contain more than one nucleus (unpublished data), indicating growth defects. In the presence of chemoattractant, small portion of WASP^{TK} cells (30%) appear to develop a pseudopod slowly in the direction of the chemoattractant gradient but the remainder of the cell body does not polarize (Figure 3A), resulting in very slow movement with a higher angular deviation due to frequent change of the direction of movement. They move at a speed of 2–3 μm/min, four times slower than wild-type cells (8–10 μm/min) as shown in Figure 3D. WASP^{TK} cells showed significantly lower chemotaxis index than wild-type cells, suggesting that their defects are due to the lack of persistence. The speed and angular deviations were recovered by the expression of tTA, a chimeric tetracycline-controlled transcriptional activator protein that results in higher expression of WASP. These cells also exhibited recovery of cellular polarity (Figure 3, A and D), indicating the necessity of WASP for cell motility and polarity. Inability of WASP^{TK} cells to chemotax efficiently was clearly manifested in the traces of cells migrating toward cAMP source (Figure 3B). Wild-type cells chemotax in a directed manner, showing straight paths of movement, whereas WASP^{TK} cells show unbiased movement indicated by higher angular deviation. To determine if the chemotaxis defects are due to a general lack of responsiveness to the chemoattractant, we examined the expression of cAR1, the major cAMP chemoattractant receptor that regulates aggregation. The expression of cAR1 was normal (unpublished data). To ensure that other signaling pathways are not altered, we examined the translocation of AktPH-GFP to the membrane upon cAMP stimulation and the kinetics of translocation in WASP^{TK} was the same as in wild-type cells (Figure 3E), indicating that pathways activating PI3 kinase are intact. Combined with normal cAR1 expression, this result suggests that other signaling pathways are not altered.

Motility Defects of Cells Expressing Low Level of WASP during Multicellular Development

To examine the effect of disrupting *WASP* on multicellular development, cells were plated on nonnutrient agar and development was examined (Figure 4). WASP^{hypo} cells exhibit a very significant motility defect during morphogenesis, remaining at the mound stage three times longer than wild-type cells. At the mound stage, the prestalk cells sort from the prespore cells by chemotaxis and differential cell adhesion, forming at tip that elongates to form the migrating

slug (Weijer, 1999; Firtel and Meili, 2000). We expect the delay at the mound stage to be due to motility defects of WASP^{hypo} cells. Similar morphogenesis defects have been demonstrated for other mutants affecting the actin-myosin cytoskeleton. The delay of development probably results from the abnormal regulation of the cytoskeletal organization, which would affect cell movement during chemotaxis and late development. At the mound stage cells differentiate into different cell types and sort themselves out to specific area of the mound due to differential adhesion and motility. The motility defect of WASP^{hypo} cells probably delays this cell sorting, which presumably prolongs the mound period. When mixed with wild-type cells, the WASP^{hypo} cells initially distribute randomly in the mound. WASP^{hypo} cells do not actively migrate into the stream of cells rotating in the mound, resulted in the exclusion of WASP^{hypo} cells to the mound periphery (Figure 4B). The motility defects are more significant in WASP^{TK} cells because they do not aggregate when starved on nonnutrient agar plates. Defects of WASP^{TK} cells can be rescued by the ectopic expression of GFP-WASP as shown in Figure 4A. WASP^{TK} cells do not effectively participate in the aggregation when they are mixed with wild-type cells and are excluded from the mound as morphogenesis ensues (Figure 4C). Wild-type cells in the mound are well elongated and polarized, but majority of WASP^{TK} cells are neither present in the mound nor well polarized, also indicating that WASP^{TK} cells do not actively chemotax. As the expression of cAMP receptor is normal and other signaling pathways are intact, we conclude that the failure to aggregate results from defects in chemotactic motility, not from an inability to respond to the chemoattractant.

Subcellular Localization of WASP in Migrating Cells

To determine if there is a dynamic subcellular localization of WASP in response to chemoattractant stimulation, we fused GFP to the N-terminus of full-length WASP, separated by a flexible linker Gly-Ser-Gly-Ser-Gly. We examined cells stably expressing moderate levels of GFP-WASP (GFP-WASP/WASP^{hypo}) and found that GFP-WASP is transiently concentrated at the leading edge and, to a lesser extent, at the uropod of *Dictyostelium* cells migrating toward a chemoattractant gradient (Figure 5A). This subcellular localization is consistent with the organization of the actin cytoskeleton indicated by phalloidin staining in migrating cells. The enrichment of GFP-WASP at the leading edge of chemotaxing cells suggests that cAMP-activated signaling pathways may regulate WASP translocation to the leading edge that, in turn, stimulates F-actin assembly.

The Basic Domain of WASP Might Be a Major Determinant for WASP Localization

The biased localization of WASP at the leading edge and uropod raises two major questions. First, is spatial localization of WASP directly correlated with the stimulation of F-actin nucleation? We attempted to answer this question by simultaneously monitoring WASP localization and F-actin assembly in live cells. We fused spectrally distinct variants of the green fluorescent protein (GFP), YFP and CFP, to WASP and to coronin, respectively, and coexpressed them in WASP^{hypo} cells. By using a high-speed excitation filter wheel, we acquired differential images of the two reporters with time-lapse microscopy. Coronin is a conserved component of the actin cytoskeleton found in all eukaryotes examined from yeast to mammals and binds specifically to F-actin and bundles of actin filaments and localizes to sites of dynamic F-actin assembly (de Hostos, 1999; Asano *et al.*, 2001). Coronin has been used as a reporter for F-actin distribution in live cells (Gerisch *et al.*, 1995). As shown in Figure 5C, newly formed pseudopodia are initially enriched with YFP-WASP and precede the localization of CFP-coronin, consistent with F-actin assembly at the leading edge being downstream from the localization and activation of WASP. The second question is: what are the determinants for WASP localization? Studies suggested that the activity of PI3 Kinase is essential for the polarized F-actin organization in migrating cells (Rickert *et al.*, 2000; Devreotes and Janetopoulos, 2003; Merlot and Firtel, 2003). The WH1 and B (basic) domains of N-WASP have been shown to mediate binding phosphatidylinositol 4,5-bisphosphate ($PI(4,5)P_2$; Miki *et al.*, 1996; Imai *et al.*, 1999), suggesting that these domains might be responsible for targeting WASP to the membrane via the interaction with the B domain. GFP-WASP lacking the WH1 and B domain displays a diffuse distribution in chemotaxing cells, suggesting that these domains are required for the dynamic regulation of WASP localization in moving cells (Figure 5A). We then expressed the GFP-fused WH1 domain and B domain linked to the GBD (GTPase binding domain; B-GBD) individually in wild-type cells to determine whether they have similar distribution to WASP. GFP-WH1 distributes uniformly in the cell, whereas GFP-B-GBD shows polarized distribution to the leading edge and uropod, indicating that the B domain is a major determinant for WASP localization. The presence of

Figure 3 (facing page). Abnormal chemotactic movement of cells expressing low levels of WASP. (A) DIC images of cells migrating toward a cAMP gradient. Wild-type cells are well polarized and retract uropod actively. WASP^{hypo} cells have defects in protruding lamellipod and retracting rear cell body, resulting in narrow and long uropod. WASP^{TK} cells do not polarize and actively migrate. WASP^{TK} cells expressing tTA, a chimeric tetracycline-controlled transcriptional activator protein, recovers normal chemotactic movements. Images of cell at 0, 7, and 14 min are shown. (B) Chemotaxis of cells were analyzed by Metamorph software (Universal Imaging) and traces of cells chemotaxing toward cAMP source are shown. Asterisk represents the position of micropipette. (C) Cell body length of WASP^{hypo} cells migrating toward cAMP gradient. Because of lack of active retraction at the uropod, the length of cell body extends until the uropod retracts by mechanical force generated by pseudopod extension. As an example, variations of cell body length of a wild-type cell and a WASP^{hypo} mutant cell are shown in the left. Differences in longest and shortest cell body lengths of eight cells during chemotaxis were analyzed and are shown in the right. (D) Chemotaxis speed of wild-type, WASP^{TK}, and WASP^{TK} cells expressing tTA ($n = 6$). The chemotactic speed of WASP^{TK} cells is significantly decreased, but recovered by the expression of tTA leading WASP expression. DIC images of migrating cells were taken in 6-s intervals for 15 min and analyzed with Metamorph software. Angular deviation shows deviations of the angle of the path taken by cells from frame to frame. Chemotaxis indices were calculated as described in Futrelle *et al.* (1982). If the cell moves directly toward the gradient source it is 1, if directly away it is -1. If movement is indifferent to gradient (random movement), it is 0. (E) Translocation of Akt/PH-GFP upon cAMP stimulation. Wild-type and WASP^{TK} cells expressing PH domain of Akt/PKB (Akt/PH-GFP) were stimulated by the addition of a saturating dose of cAMP (10 μM). On cAMP stimulation, a dramatic translocation of Akt/PH-GFP from the cytosol to the plasma membrane is observed. Numbers in the lower right corner are seconds before and after stimulation. Right panel shows the translocation kinetics of Akt/PH-GFP obtained from time-lapse recordings. The fluorescence intensity of membrane-localized GFP fusion protein was quantitated as E(t) using the linescan module of Metamorph software (Universal Imaging). Et/Eo is plotted as a measure of the amount of membrane-associated protein relative to the starting conditions.

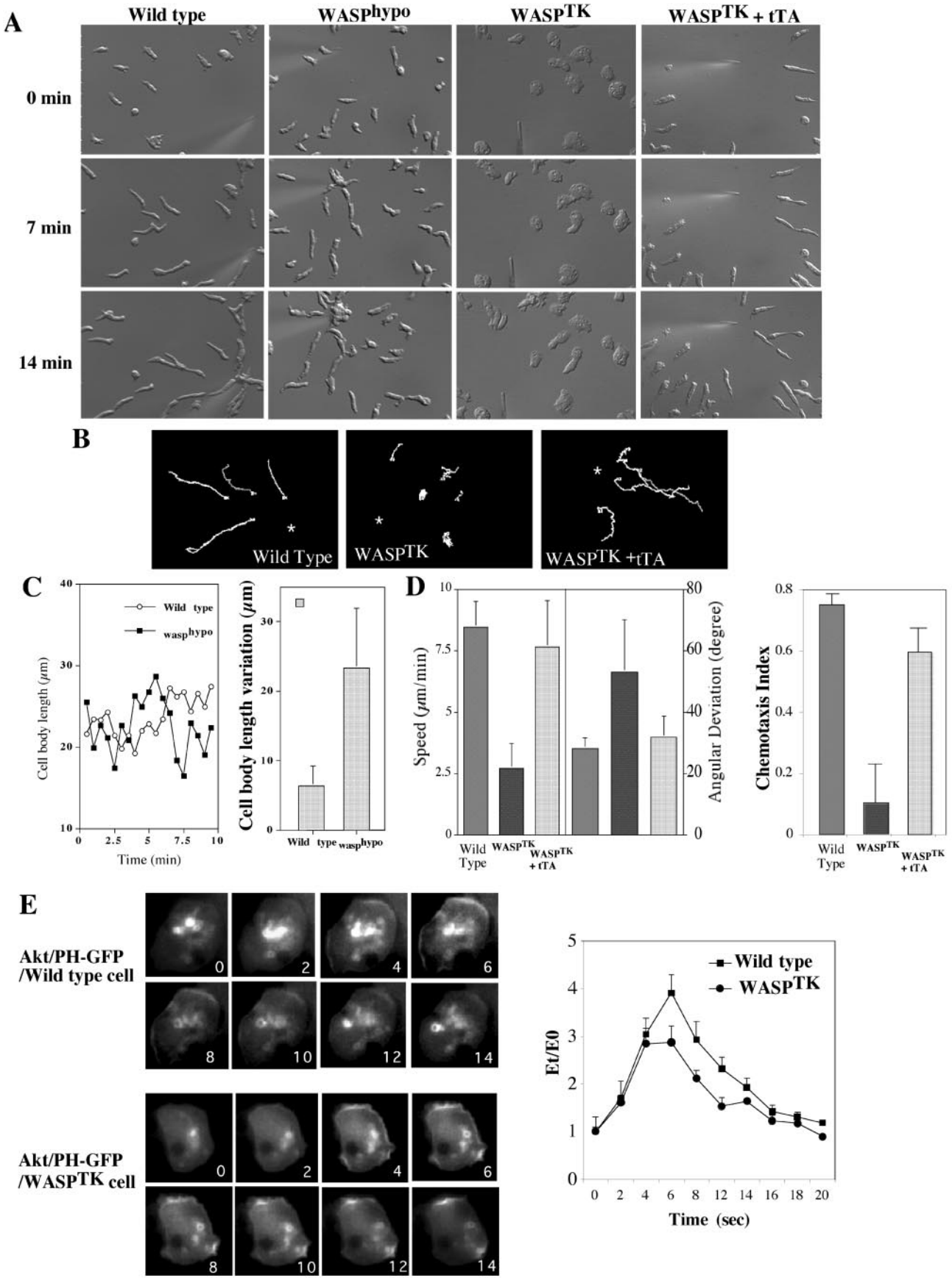
A
Wild type
WASPhypo
WASPTK
WASPTK + tTA
0 min
7 min
14 min
B
Wild Type
WASPTK
WASPTK +tTA
C
Wild type
wasphypo
Cell body length (μm)
Time (min)
Cell body length variation (μm)
Wild type
wasphypo
D
Speed (μm/min)
Angular Deviation (degree)
Wild Type
WASPTK
WASPTK + tTA
Chemotaxis Index
Wild Type
WASPTK
WASPTK + tTA
E
Akt/PH-GFP /Wild type cell
Akt/PH-GFP /WASPTK cell
Wild type
WASPTK
Et/E0
Time (sec)

Figure 3.

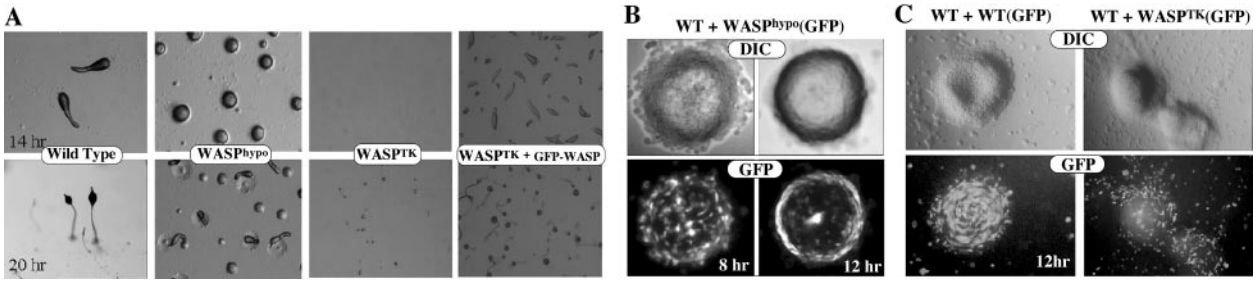

Figure 4. Motility defects of cells expressing low level of WASP in multicellular development. (A) Development of cells expressing a low level of WASP. Cells grown in axenic medium were washed and plated on nonnutrient agar plate. Photographs were taken at various developmental stages thereafter. Development of $WASP^{hypo}$ cells was delayed in mound stage, resulting in delayed formation of slugs and fruiting bodies. $WASP^{TK}$ cells showed a severe defect in chemotactic aggregation, resulting in few fruits formed. Ectopic expression of GFP-WASP rescued defects of $WASP^{TK}$ cells. (B) Motility defect of $WASP^{hypo}$ cells. Wild-type, $WASP^{hypo}$, $WASP^{hypo}$ cells expressing GFP were mixed in a ratio of 8:1:1. GFP-labeled $WASP^{hypo}$ cells were uniformly distributed in the loose-aggregate at 8 h after the onset of development, but sorted out to the periphery of the tight mound (12 h), presumably due to the motility defect. (C) Motility defects of $WASP^{TK}$ cells. GFP-labeled $WASP^{TK}$ cells were mixed with unlabeled wild-type cells, and they showed significant defects in chemotactic aggregation. Most of GFP-labeled $WASP^{TK}$ cells were neither present in the mound nor polarized.

GBD domain might be required, but not sufficient for the localization of WASP (unpublished data). Interestingly, GFP-B-GBD appeared to be associated with vesicle-like structures as revealed by punctate pattern of GFP signal at the leading edge and uropod, which is different from more diffuse distribution of GFP-WASP. To test if more diffuse distribution of GFP-WASP is due to higher expression level, we expressed GFP-WASP in $WASP^{TK}$ cells. GFP-WASP still shows biased distribution at the leading edge and uropod, but GFP-WASP indeed showed punctate vesicle localization at the leading edge and uropod (Figure 5B). Higher expression of GFP-WASP in $WASP^{TK}$ cells showed more diffuse distribution presumably because binding sites on vesicles are saturated.

The Basic Domain Has a Broader Specificity to Phosphoinositides

Previous reports have suggested that the B domain is important for binding $PI(4,5)P_2$, which is thought to be involved with relieving the autoinhibited conformational state of WASP (Higgs and Pollard, 2000; Prehoda *et al.*, 2000; Rohatgi *et al.*, 2000). However, the range of phosphoinositide species capable of binding this domain has not been determined thoroughly. To gain a better understanding of the profile of phosphoinositides capable of binding the B domain of WASP, we used a protein–lipid overlay assay previously used to determine specific phosphoinositide binding by the pleckstrin homology (PH) domain (Deak *et al.*, 1999). This takes advantage of commercially available PIP-Strips (Echelon), which consist of phospholipids immobilized onto nitrocellulose. The PIP strips were incubated with purified GST-B-GBD or GST-WH1-B-GBD fusion proteins and the binding was determined by conventional Western blotting with an anti-GST antibody. As a positive control, we used a GST-fusion of PH domain of human PLCδ1, which has been known to have a strong specificity to $PI(4,5)P_2$ and it showed strong preference to $PI(4,5)P_2$. Both WH1-B-GBD and GST-B-GBD fusion proteins showed significant binding to three phosphatidylinositol lipids, $PI(3,4)P_2$, $PI(3,5)P_2$, and $PI(3,4,5)P_3$, but moderate binding to $PI(4,5)P_2$ (Figure 6A). The absolute binding intensity of GST-B-GBD to $PI(3,4,5)P_3$ is similar to that of PLCδPH to $PI(4,5)P_2$. However, GST-B-GBD had higher background binding to membrane than PLCδPH, presumably due to the difference of affinity. To show specific binding intensity, we subtracted the background intensity from the absolute intensity, which results in relatively low binding intensity of GST-B-GBD. GST and GST-WH1 did not show specific binding to any of phospholipids on the strip (unpublished data). The binding of GST-B-GBD protein to $PI(3,4,5)P_3$ was also confirmed by a protein pull-down experiment using PIP beads (Echelon). GST-B-GBD showed binding to $PI(3,4,5)P_3$-beads with slightly higher affinity than to $PI(4,5)P_2$-beads, whereas control beads show minimal binding (Figure 6B). To verify specific binding of phosphoinositides to the B-GBD domain of WASP in a more physiological condition, we performed a liposome cosedimentation assay with purified GST-YFP-B-GBD protein and liposomes composed of 95% of phosphatidylcholine (PC) and 5% of either PI, PI(4)P, $PI(4,5)P_2$, or $PI(3,4,5)P_3$. Binding of the B-GBD domain to a specific phosphoinositide would result in the sedimentation of a protein–liposome complex that can be recovered at a higher concentration of Optiprep (Greiner) fractions. GST-YFP-B-GBD proteins and liposomes were mixed and subjected to centrifugation on a Optiprep gradient (5–30% Optiprep). Fractions were collected and resolved on SDS-PAGE gel and GST-YFP-B-GBD protein was probed by a Western blot. As presented in Figure 6C, GST-YFP-B-GBD protein mixed with liposome composed entirely of PC or liposomes containing 5% PI and PI(4)P was found in lower Optiprep concentration fractions, indicating little binding of B-GBD to PC, PI, and PI(4)P. With liposomes containing 5% $PI(3,4,5)P_3$ and $PI(4,5)P_2$, GST-YFP-B-GBD was found at the higher (~30% Optiprep) concentration of gradient, indicating that B-GBD domain bound with higher affinity to $PI(3,4,5)P_3$ and $PI(4,5)P_2$. Ovalbumin was added in the binding mixture to block nonspecific binding, and it also serves as an internal control for lower concentrations of Optiprep fraction. We quantified specific binding efficiency by summing of protein band intensity in the higher fractions than fractions where ovalbumin was present (Figure 6C). The binding efficiency of B-GBD domain was almost equal to $PI(3,4,5)P_3$ and $PI(4,5)P_2$ and was significantly higher than to PI, PI(4)P, and PC. We examined the binding specificity of GST-WASP to phosphoinositides and also found preference to $PI(3,4,5)P_3$ or $PI(4,5)P_2$ but not as significant as the B domain. This is presumably due to the autoinhibitory conformation of WASP requiring Cdc42 or Rac to bind to the GBD domain for full activation. Together these experiments suggest that the B domain has a more diverse phospholipid binding

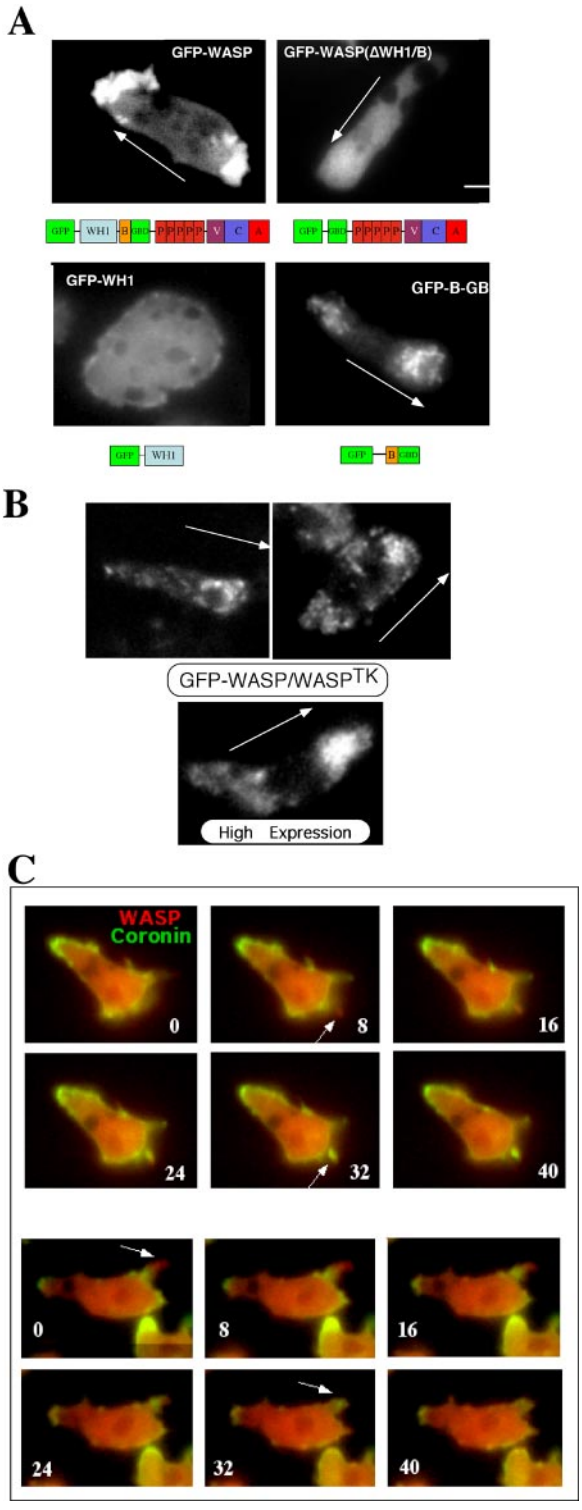

Figure 5. (A) Localization of GFP-WASP in *Dictyostelium* cells ($WASP^{hypo}$) migrating toward a cAMP gradient. For examining GFP-WASP, cells were pulsed for 4.5 h at 6-min intervals. Fluorescence images were taken from live aggregation-competent cells migrating toward a chemoattractant gradient. GFP-WASP localizes to the leading edge and the uropod, which is recapitulated by GFP-B-GBD. GFP-WASP variant lacking WH1-B domains do not show prominent localization because GFP-WH1 shows uniform distribution. Arrows indicate the direction of gradient. Bar, 5 μm. (B) Localization of GFP-WASP in $WASP^{TK}$ cells. GFP-WASP still shows biased distribution at the leading edge and uropod, but

profile than implied by previous reports and that the interaction of the B domain with $PI(3,4,5)P_3$ is important for the localization and activation of WASP to the leading edge of chemotaxing cells. To confirm if PI3K is required for the localization of WASP and F-actin polymerization at the leading edge, we used the PI3K inhibitor LY294002 and examined the localization of GFP-coronin and YFP-WASP. Before LY294002 addition, GFP-coronin, and therefore F-actin, is highly localized to the leading edge of chemotaxing cells (Figure 6D). Addition of LY294002 to polarized cells results in a loss of the polarized actin cytoskeleton as determined by a rapid loss of the localization of GFP-coronin. Similarly, addition of LY294002 to polarized cells cause rapid loss of the polarized distribution of GFP-WASP and uniform distribution of GFP-WASP in the cytoplasm, suggesting that PI3K activity is essential for maintaining polarized F-actin assembly and WASP localization. It should be noted that the redistribution of WASP upon LY294002 treatment is slower than that of coronin, which might be due to the association of WASP with vesicles that might be tethered to microtubules or diffusing significantly slower. These results strongly suggest that the interaction of the B domain with $PI(3,4,5)P_3$ is important for the localization and activation of WASP to the leading edge of chemotaxing cells. Interactions of B domain with $PI(4,5)P_2$ and $PI(3,4,5)P_3$ in lipid binding assays prompted us to examine the colocalization of YFP-B-GBD with CFP-PLCδ1PH, a probe for $PI(4,5)P_2$ in chemotaxing cells by performing time-lapse microscopy (Figure 7A). Surprisingly, CFP-PLCδ1PH primarily showed punctate vesicle labeling similar to localization of YFP-B-GBD and CFP-PLCδ1PH and YFP-B-GBD appeared to colocalize on many vesicles. The distribution of these PIP2-enriched vesicles somewhat polarized because vesicles mainly showed biased distribution at the leading edge and uropod area, but few vesicles labeled with CFP-PLCδ1PH can be found at the proximity of the leading edge membrane. However, YFP-B-GBD signal was found at the leading edge and not colocalized with CFP-PLCδ1PH. To determine if YFP-B-GBD localizes to the $PI(3,4,5)P_3$-enriched membrane, we examined the colocalization of YFP-B-GBD and CFP-PhdA which selectively binds to $PI(3,4,5)P_3$ (Funamoto *et al.*, 2001; Figure 7B). CFP-PhdA temporarily localizes to the leading edge of chemotaxing cells, but hardly showed association with intracellular vesicles. Most of YFP-B-GBD signal were associated with vesicles, but some of YFP-B-GBD signal clearly colocalizes with CFP-PhdA at the leading edge, indicating that the B domain is recruited to the membrane where local $PI(3,4,5)P_3$ concentration is elevated by the activation of PI3 kinase.

The B domain of WASP is highly enriched in positively charged Lys residues. To determine which residues might be important for phospholipid binding, we mutated these Lys to Ala residues and the specificity of each mutant was tested with the lipid overlay assay (Figure 7C). Surprisingly, only two mutations significantly hampered the binding of GST-B-GBD to phosphoinositides. Mutation on Lys^{156} to Ala

Figure 5 (cont). appears to be associated with vesicular structures. Higher expression of GFP-WASP showed more diffuse distribution. (C) Localization of YFP-WASP to the leading edge. CFP-Coronin and YFP-WASP were coexpressed in $wasp^{hypo}$ cells, and their localizations in chemotaxing cells were examined in time-lapse recording of alternate exposures (1 s) for CFP and YFP. Images were acquired and analyzed with multidimensional acquisition utility of Metamorph (Universal Imaging) software. Coronin localizes to sites of dynamic actin assembly and functions as a reporter for F-actin distribution in live cells.

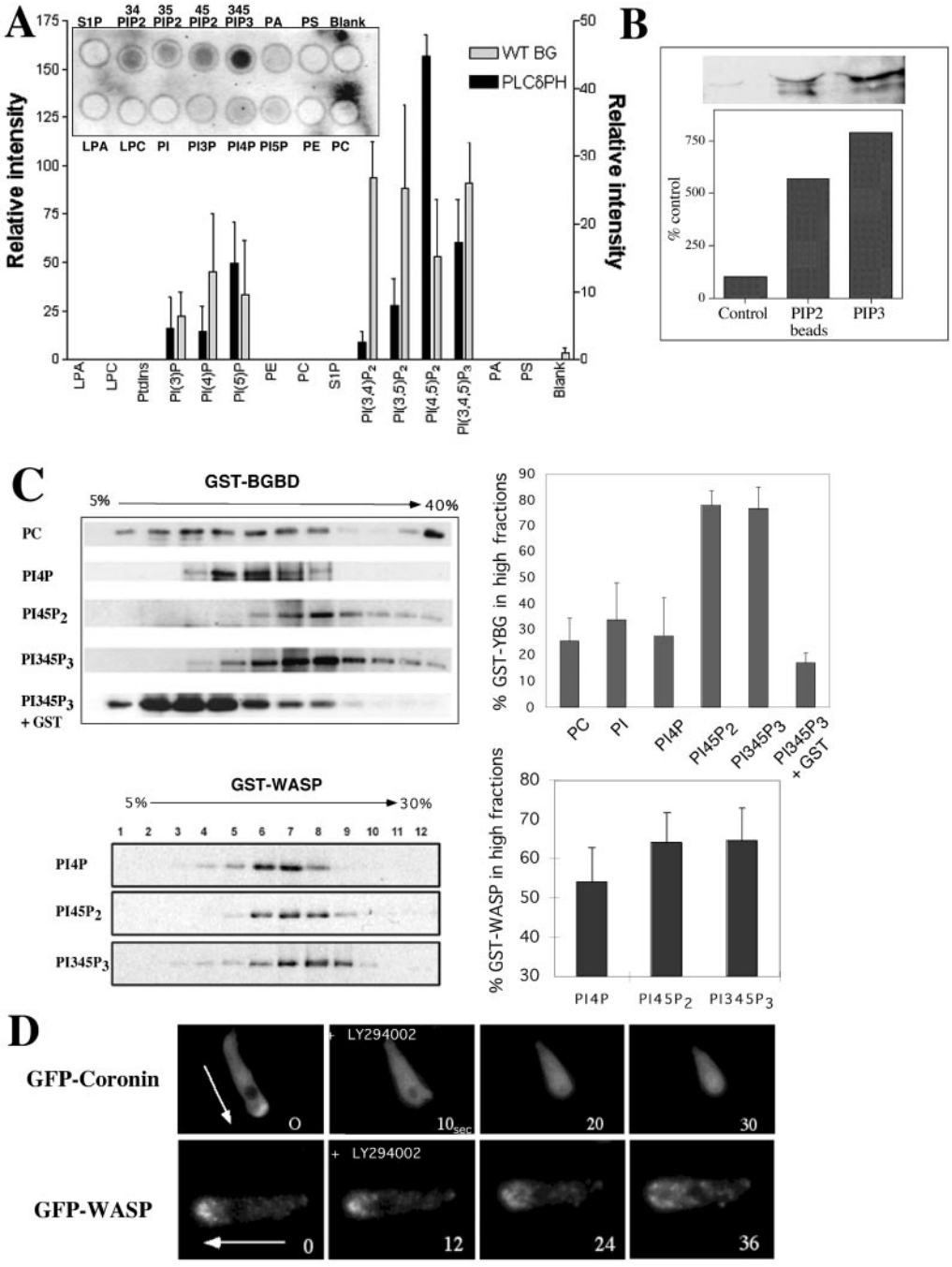

Figure 6. (A) The phospholipid binding properties of the basic domain of WASP. The indicated phospholipids were spotted onto a nitrocellulose membrane (PIP strip) that was then incubated with GST-PH/PLCδ1 and GST-B-GBD. The membranes were washed and the GST fusion proteins bound were detected by Western blot using a GST antibody. Inset shows a PIP strip and bar graph is an average of four PIP strips. Note that GST-PH/PLCδ1 specifically bound to $PI(4,5)P_2$, but GST-B-GBD showed higher affinity to $PI(3,4,5)P_3$ and $PI(3,4)P_2$, which are products of PI3 kinase. Unexpectedly higher binding to PI(4)P and PI(5)P in the graph was due to having one blot showing unusually high binding to PI(4)P and PI(5)P. (B) PIP beads pull-down assay. GST-B-GBD fusion protein was incubated with agarose beads cross-linked to phosphoinositides and bound GST-fusion protein was pulled down and then probed by a Western blot. GST-B-GBD showed binding to $PI(3,4,5)P_3$-beads with slightly higher affinity than to $PI(4,5)P_2$-beads, whereas control beads showed minimal binding. Quantification of three experiments is shown. (C) Liposome cosedimentation assay with purified GST-YFP-B-GBD or GST-WASP protein and liposomes composed of 95% PC and 5% of either PI, PI(4)P, $PI(4,5)P_2$, or $PI(3,4,5)P_3$. GST-YFP-B-GBD protein and liposomes were mixed and subjected to centrifugation on an Optiprep gradient (5–30% Optiprep). Collected fractions were run on SDS-PAGE gel and probed with Western blot with anti-GST antibody. Ovalbumin was added in the binding mixture to block nonspecific binding and it also serves as an internal control for lower concentration of Optiprep fraction. Specific binding efficiency was quantified by summing of GST-YFP-B-GBD band intensity in the higher fractions than fractions where ovalbumin was present. (D) Disruption of polarized localization of GFP-WASP by the PI3K inhibitor LY294002. *Dictyostelium* chemotaxing cells expressing the Coronin-GFP or GFP-WASP were treated with 15 μM LY294002 and the change in the subcellular localization of Coronin-GFP and GFP-WASP was followed by time-lapse digital video microscopy. Arrows indicate the direction of movements and numbers shown are time (seconds) after LY treatment.

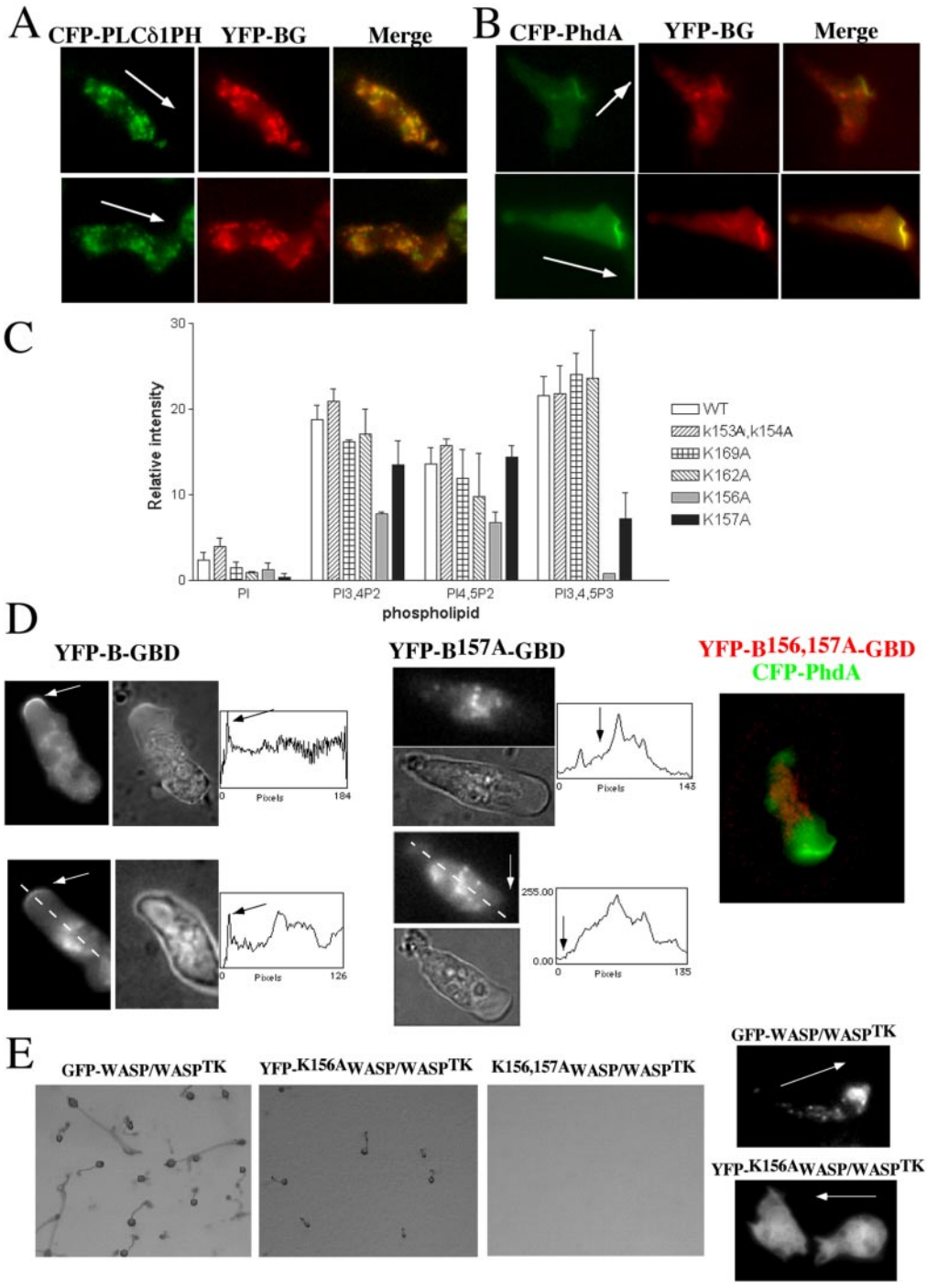

Figure 7. (A) Colocalization of YFP-B-GBD and CFP-PLCδ1PH in chemotaxing cells. CFP-PLCδ1PH binds to $PI(4,5)P_2$ with very high specificity. CFP-PLCδ1PH showed punctate vesicle labeling, which appears to overlap with the YFP-B-GBD signal. Note that some YFP-B-GBD signal was found at the leading edge without colocalization with CFP-PLCδ1PH. (B) Colocalization of YFP-B-GBD and CFP-PhdA in chemotaxing cells. CFP-PhdA selectively binds to $PI(3,4,5)P_3$ and accumulated at the leading edge of migrating cells. Wild-type cells migrating toward a cAMP source show a distinct colocalization of PhdA–GFP and YFP-B-GBD at the leading edge. (C) PIP strip assay of B domain mutants. Lys residues of the B domain were mutated to Ala and the binding efficiency of the GST fusion protein of these mutants to phosphoinositides were assessed by PIP strip assay. Lys^{156A} and Lys^{157A} appear to specifically block the binding to phosphoinositides. (D) Localization of YFP-B-GBD and YFP-B^{157A}-GBD in chemotaxing cells. Phase contrast and fluorescence micrographs of cells expressing YFP-B-GBD and YFP-B^{157A}-GBD are shown. Note that the YFP-B-GBD is localized at the leading edge, but the localization of YFP-B^{157A}-GBD to the leading edge is significantly reduced. Fluorescence intensities of YFP were measured along a thin line through the central portion of the cell. Arrows indicate the position of the leading edge. Some of YFP-B-GBD signal was from intracellular vesicles, which appears to be blurry because optical focus was at the leading edge membrane, which cells tend to lift up. YFP-$B^{156,157A}$-GBD showed essentially the same distribution as YFP-B^{157A}-GBD. (E) Rescue of motility defects of $WASP^{TK}$ cells by expressing WASP B domain mutants. Wild-type WASP, ^{K156A}WASP, or ^{K156,157A}WASP were expressed in $WASP^{TK}$cells and their development were examined. Cells expressing ^{K156A}WASP showed partial rescue of development, whereas ^{K156,157A}WASP did not rescue motility defects of $WASP^{TK}$ cells. Compared with polarized localization of GFP-WASP, YFP-^{K156A}WASP did not show any biased localization.

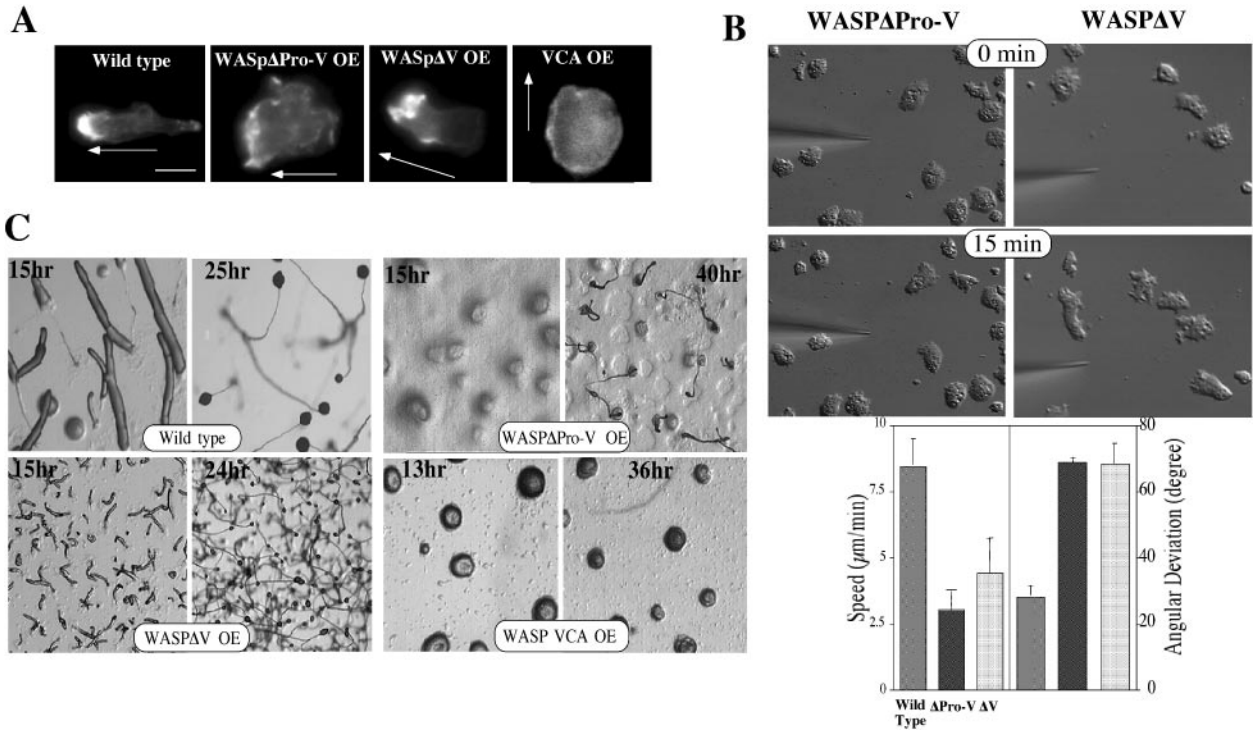

Figure 8. F-actin organization of cells expressing WASP mutants. (A) Deletion mutations expected to abrogate the function of specific domains of WASP were created and F-actin organization of cells expressing these mutants were examined by TRITC-phalloidin staining. Cells under a cAMP gradient were fixed and stained with TRITC-phalloidin. Arrows indicate the direction of gradient. (B) Chemotaxis of cells expressing WASPΔProV and GFP-WASPΔV. DIC images of cells migrating toward a cAMP gradient at 0 and 15 min are shown. Average speed and angular deviation of these mutants are shown. (C) Developmental phenotypes of cells expressing WASP truncation mutants. Cells grown in axenic medium were washed and plated on nonnutrient agar plate. Photographs were taken at various developmental stages thereafter.

appears to be important for binding all three phosphoinositides tested (PI(3,4)P_2, PI(4,5)P_2, PI(3,4,5)P_3), whereas mutation of lysine 157 reduces binding to those lipids with a phosphate at the 3′ position (PI(3,4)P_2 and PI(3,4,5)P_3), suggesting Lys^{157} is important for an interaction with 3′-position phosphate. The selective reduction of this mutant to phosphoinositide with the 3′ position phosphate further validates the specificity of binding of the B domain to PI(3,4,5)P_3.

Because mutations on Lys^{157A} specifically reduced the binding of B domain to PI(3,4,5)P_3, we compared the intracellular localization of the YFP-B-GBD with the YFP-B^{157A}-GBD mutant to determine whether Lys^{157} residue is important for the localization of YFP-B-GBD to the leading edge. Highly polarized, chemotaxing cells exhibit YFP-B-GBD localization at the leading edge. Mutation of Lys^{157} to Ala appears to decrease YFP-B-GBD localization at the leading edge of polarized cells, but did not significantly affect the association of YFP-B-GBD with intracellular vesicles (Figure 7D). YFP-$B^{156,157A}$-GBD showed essentially the same distribution as YFP-B^{157A}-GBD. These results strongly suggest that the interaction of the B domain with PI(3,4,5)P_3 is important for the localization and activation of WASP to the leading edge of chemotaxing cells. We further elucidated the functional significance of these mutations in the B domain by determining if WASP carrying these mutations is able to rescue the phenotype of $WASP^{TK}$. ^{K156A}WASP expressed in $WASP^{TK}$ minimally rescued chemotaxis defects (Figure 7E) but ^{K156,157A}WASP failed to rescue the phenotype of $WASP^{TK}$. YFP-^{K156A}WASP did not show any preferential localization in the cell nor showed punctate vesicular distribution.

WASP Subdomain Deletion Mutants

We created deletion mutations that are expected to abrogate the function of specific domains of WASP. Cells overexpressing the WASP VCA domain, which stimulates F-actin nucleation activity in vitro in association with the Arp2/3 complex (Machesky and Insall, 1998), are not well polarized compared with wild-type cells and do not exhibit a prominent F-actin–rich cortical region with phalloidin staining of starved cells (Figure 8A). This presumably results from the nonlocalized and unregulated nucleation of F-actin. This result is consistent with a previous study demonstrating that overexpression of carboxy-terminal fragments of SCAR1 or WASP in cells caused a disruption in the localization of the Arp2/3 complex and, concomitantly, induced a complete loss of lamellipodia and actin spots (Machesky and Insall, 1998). The poly-proline domain of mammalian WASP binds a number of SH3 domain–containing proteins (Badour *et al.*, 2003). Mutations within this domain of human WASP result in a severe WAS phenotype (Ochs, 1998a), indicating that the poly-proline region plays an important role in the regulation of WASP function. *Dictyostelium* cells expressing a WASP construct lacking the whole polyproline region and the V domain (WASPΔProV) exhibit no polarized F-actin organization and up-regulated cortical F-actin filaments along the periphery of cells under the gradient (Figure 8A). These cells, not unexpectedly, have severe defects in the ability to polarize and chemotax in a response to a chemoat-

tractant gradient (Figure 8B). Cells overexpressing WASPΔProV do not polarize nor extend pseudopodia effectively, probably because they lack dynamic regulation of the F-actin cytoskeleton. In contrast, cells expressing WASP lacking the last two polyproline repeats and the V domain (WASPΔV) have polarized F-actin organization and extend pseudopodia toward the cAMP gradient and show some polarization, although not to the extent as wild-type cells (Figure 8, A and B). Defects of chemotactic movement of these mutants are also manifested in the development of these mutants (Figure 8C). Cells expressing WASPΔProV did not aggregate, even after 24 h, consistent with an inability to chemotax. However, cells expressing WASPΔV aggregate through limited chemotaxis and cell-cell adhesion with neighboring cells to form many small mounds, which eventually develop into small fruiting bodies. These results suggest that the poly-proline region of WASP and its presumed interaction with SH3 domain–containing proteins might play an important role in controlling WASP function and localization and thus, polarized F-actin organization.

DISCUSSION

The actin cytoskeleton controls the overall structure of cells and is highly polarized in chemotaxing cells, with F-actin localized predominantly in the anterior leading edge and to a lesser degree in the cell's posterior (Gerisch *et al.,* 1995; Parent *et al.,* 1998; Borisy and Svitkina, 2000; Firtel and Chung, 2000). In the present study, we demonstrated the specific and essential role of WASP in organizing polarized F-actin assembly in chemotaxing *Dictyostelium* cells. WASP^{TK} cells, which express very low levels of WASP, show reduced F-actin levels in unstimulated cells and significant defects in polarized F-actin assembly in migrating cells in response to chemoattractant stimulation. These cells are unable to establish axial polarity in the chemoattractant gradient and their motility is also severely impaired. The lack of an F-actin–enriched lamellipodia and uropod in WASP^{TK} cells in a cAMP gradient indicates that WASP is essential for polarized assembly of F-actin. Our studies are consistent with the findings that macrophages from WAS patients are less persistent in their locomotion and engage in more frequent turning behavior compared with normal counterparts (Thrasher *et al.,* 2000). Lack of cell polarization and maintaining directional cues in WAS macrophage may underlie the failure of these cells to migrate normally. Induction of monocyte chemotaxis by chemokines is preceded by cell polarization, marked by several morphological changes, including the formation of cell protrusions and pseudopodia. Staining of F-actin in monocytes from WAS patients stimulated with chemoattractants shows a severe defect in cell polarization after stimulation with either FMLP or MCP-1 compared with the response of monocytes from normal donors (Badolato *et al.,* 1998). Bee1, a yeast homologue of WASP, has been implicated in the regulation of cellular polarity as it is involved in the formation of actin patches. The lack of cortical patches in *bee1* cells suggests that disruption of cortical patches slows down polarized cell surface growth and cytokinesis (Li, 1997). IL-4 and anti-CD40 induction of B cell polarization from WASP deficient mice was impaired in comparison to WASP+ cells(Westerberg *et al.,* 2001). Interestingly, N-WASP was clearly detected in both WASP+ and WASP- B cells, in similar concentrations, indicating that they regulate different processes despite the high degree of homology.

Our data also suggest that WASP and SCAR might be controlled by different signaling pathways, leading F-actin assembly for different cellular processes. WASP might be more important in the regulation of cell polarity than SCAR because WASP^{TK} cells showed significant lack of cell polarity and aggregation, whereas *scar* null cells become polarized, roughly orienting toward the aggregation center and forming visible aggregation streams (Bear *et al.,* 1998). *Dictyostelium* WASP is more closely related to the mammalian WASP that is only expressed in hematopoietic cells. It is conceivable that WASP function in highly motile cells such as *Dictyostelium,* neutrophils, and macrophages is more essential than SCAR in order to provide highly dynamic regulation of actin cytoskeleton. Thus, lack of WASP function might cause more severe phenotypes in highly motile cells. Recent studies in *Drosophila* have shown that WASP is largely dispensable for Arp2/3-dependent control of dynamically regulated actin structures including cortical F-actin, whereas SCAR does not contribute to cell fate decisions in which WASP and Arp2/3 play an essential role (Zallen *et al.,* 2002). Further, it has been demonstrated that the VCA domain of SCAR shows different potency in stimulating Arp2/3 than that of WASP or N-WASP, at least in in vitro systems. In a bead motility assay, the minimal region of WASP sufficient to direct movement of beads was the C-terminal VCA fragment, whereas the corresponding region of SCAR1 was insufficient (Yarar *et al.,* 2002). VCA domains of WASP, N-WASP, and SCAR1 were found to bind actin and Arp2/3 with nearly identical affinities but to induce unique kinetics of actin assembly (Zalevsky *et al.,* 2001). N-WASP and WASP induce rapid actin polymerization, while SCAR1 either fails to induce detectable polymerization or to induce the slowest rate of nucleation. Based on these results, it is conceivable to expect WASP or N-WASP to be the primary regulators of dynamic F-actin assembly. It is clear that differential activation of Arp2/3 complex would be required for regulation of cellular processes as it has been suggested that different rates of filament formation may help determine the architecture of actin networks produced by different nucleation-promoting factors (Zalevsky *et al.,* 2001).

Our data are the first demonstration that GFP-WASP preferentially localizes at the leading edge and uropod of chemotaxing cells and B domain is required for the localization of WASP via binding to phosphoinositides. We show that WASP lacking the WH1 and B domains is cytosolic as is a GFP-WH1 domain fusion. We further show that a GFP-B-GBD fusion shows the same leading edge and to a lesser degree uropod localization, as does full-length WASP. Combined, these data are consistent with an essential role for the B domain in the localization. The subcellular localization of WASP is consistent with the organization of the actin cytoskeleton shown by phalloidin staining and localization of CFP-coronin in migrating cells. It was rather unexpected to observe that either GFP-WASP or YFP-B-GBD are associated with vesicles that can be labeled with CFP-PLCδ1PH, indicating that vesicles are enriched with PI(4,5)P_2. The recruitment of N-WASP to the PI(4,5)P_2-enriched vesicles has been previously demonstrated and mutational analysis of N-WASP has demonstrated that WH1, B, and polyproline domains are capable of interaction with the PI(4,5)P_2 vesicles (Benesch *et al.,* 2002). The vesicular targeting of the polyproline domain was suggested to be mediated through the interactions with SH3 domain–containing proteins. The recruitment of GFP-WASP to intracellular vesicles in *Dictyostelium* might also require SH3 domain–containing proteins as N-WASP requires Nck and WIP. However, B domain must play a major role for vesicle recruitment because we observed the association of YFP-B-GBD with vesicles. It is

not clear how chemotaxing cells control biased distribution of these vesicles.

Previous studies demonstrated that the B domain of WASP interacts with PI(4,5)P_2 (Higgs and Pollard, 2000; Rohatgi *et al.*, 2000), resulting in the activation of N-WASP by changing its conformation from auto-inhibited to active (Prehoda *et al.*, 2000). The auto-inhibited conformation is acquired and maintained by the binding of the autoinhibitory region near the GBD domain to C region of the VCA domain. However, subcellular distribution of PI(4,5)P_2 has not been extensively examined in chemotaxing cells, but it has been suggested that PI(4,5)P_2 acts permissively, restricting new F-actin polymerization to the region of the plasma membrane (Insall and Weiner, 2001). In the present study, we demonstrated that the B domain has an equal or higher affinity to PI(3,4,5)P_3 than PI(4,5)P_2 in lipid-binding assays and that a mutation on Lys^{157} residue in the B domain specifically reduces the binding to PI(3,4,5)P_3 and the localization of the B domain to the leading edge membrane without hampering the association of YFP-B-GBD with vesicles enriched with PI(4,5)P_2. Our results suggest a very interesting possibility that B domain directs the localization of WASP to vesicles via interaction with PI(4,5)P_2, but the interaction of the B domain with PI(3,4,5)P_3 is required for the localization of WASP to the leading edge where vigorous F-actin polymerization occurs. In a previous study, it has been shown that inhibiting PI3K in polarized, chemotaxing cells through the addition of LY294002 results in a loss of the polarized actin cytoskeleton (Chung *et al.*, 2001). Reduced polarized F-actin organization in cells lacking two of the five class I PI3K isoforms in *Dictyostelium pi3k1/2* null cells or cells treated with LY294002 (Chung *et al.*, 2001; Funamoto *et al.*, 2001; Takeda and Firtel, unpublished data) is consistent with PI3 kinase playing an important role in the regulation of the actin cytoskeleton in chemotaxing cells, possibly through the control of WASP. PI(3,4)P_2 and PI(3,4,5)P_3 produced by PI3 kinase activity function as docking sites for diverse PH domain–containing proteins (Parent *et al.*, 1998; Meili *et al.*, 1999; Servant *et al.*, 2000; Funamoto *et al.*, 2001). We suggest that the localization of WASP to the membrane of the leading edge where active F-actin polymerization occurs requires the formation of PI(3,4,5)P_3-enriched domains, which would provide docking sites for the WASP B domain. In a recent study, binding of WAVE2 to PI(3,4,5)P_3 through its basic domain was demonstrated to be important for the localization of WAVE2 to the lamellipodia of cells stimulated with platelet-derived growth factor (Oikawa *et al.*, 2004), also suggesting a comparable linkage between PI3 kinase and regulation of WAVE2 localization. Local activation of WASP at the leading edge can be achieved by interaction with PI(3,4,5)P_3 and/or locally activated Rac molecules. Although a previous study (Funamoto *et al.*, 2002) suggested that PI3 Kinase is only enriched at the leading edge, more recent studies using more sensitive imagining suggest that PI3 Kinase also shows an enrichment in the uropod, although the level of PI3 Kinase in the uropod is significantly less than at the leading edge (Lee and Firtel, unpublished observations). Thus, PI3 Kinase may also control WASP localization to the uropod as well as to the leading edge. Both in *Dictyostelium* and neutrophil, signaling asymmetry including the activation of PI3 kinase can be achieved in the absence of F-actin polymerization (Parent *et al.*, 1998; Wang *et al.*, 2002). We demonstrated that the translocation of Akt/PH-GFP to the membrane of $WASP^{TK}$ cells upon cAMP stimulation and the kinetics of translocation was not altered, indicating that signaling pathways for polarity are intact. Reciprocal interplay between PI(3,4,5)P_3 and actin polymerization appears to be required for maintaining the asymmetry of intracellular signals responsible for cell polarity and directed motility because amplification of the internal PtdIns(3,4,5)P_3 gradient is markedly impaired by agents inhibiting actin polymerization (Wang *et al.*, 2002). Thus, polarity defects of $WASP^{TK}$ cells might be caused by the defects in persistence in cell polarity because of the lack of the sustained stimulation of F-actin polymerization. This hypothesis is consistent with our observation that the interaction of the B domain with PI(3,4,5)P_3 is required for the targeting of WASP to the leading edge membrane.

The presence of a poly-proline region in all WASP family proteins (WASP, N-WASP, and SCAR/WAVE) and identification of many SH3 domain–containing proteins as binding partners for the poly-proline region in mammalian cells suggests that the interaction between the poly-proline region and SH3 domain–containing protein(s) might play an important role in the regulation of WASP function and localization. Furthermore, previous studies show that mutations within the SH3-binding domain of WASP result in a severe WAS phenotype (Ochs, 1998). We demonstrated that cells overexpressing WASPΔProV are not polarized and cannot extend pseudopodia effectively because of aberrant regulation of F-actin organization, and cells overexpressing DdWASPΔV exhibited similar but less severe defects in polarity and chemotaxis. It was unexpected to observe a strong phenotype resulting from these mutants because they cannot stimulate F-actin nucleation due to the lack of V domain. Mutational analysis demonstrated that both WH1- and polyproline-dependent interactions of N-WASP with WIP and SH3 domain–containing proteins contribute to recruitment of N-WASP to the PI(4,5)P_2 vesicle surface (Benesch *et al.*, 2002). In a yeast two-hybrid assay, WASPΔV can interact with SH3 domains of human Nck that is known to interact with the poly-proline region of WASP (Chung and Firtel, unpublished observations), but WASPΔProV cannot. The phenotypic differences between these two mutants might result from the polyproline repeats interacting with SH3 domain-containing proteins that are possibly acting as an adaptor for other components required for general targeting of WASP to the leading edge area. More precise targeting of WASP to the membrane of the leading edge might be acquired by the interaction of the B domain with PI(3,4,5)P_3. It has been shown that the proline-rich regions of WASP and SCAR1 and the WH1 domain of WASP independently enhanced motility rates of beads in the beads motility assays (Yarar *et al.*, 2002). The contributions of these regions to motility could not be accounted for by their direct effects on actin nucleation with the Arp2/3 complex, suggesting that they stimulate motility by recruiting additional factors. WASPΔProV and WASPΔV may cause dominant negative effect due to inability to recruit additional factors or by sequestering signaling proteins in nonfunctional complexes. A recent study demonstrated that two of the SH3 domain–containing ligands, SlaI and Bbc1, cooperate to inhibit Las17, a yeast homologue of WASP, activity in vitro and are required for a shared function in actin organization in vivo (Rodal *et al.*, 2003). Moreover, a recent article demonstrated that N-WASP is predominantly present as an inactive complex with WIP whose polyproline domain presumably binds to WH1 domain of WASP (Ho *et al.*, 2004). *Dictyostelium* has a homologue of WIP (Han and Chung, unpublished observations) and expression of WASPΔProV might disrupt this multiprotein complex resulting in aberrant regulation of WASP activity.

In the future, it will be important to examine how PI(3,4,5)P_3 induces translocation of WASP from vesicles to

the leading edge membrane and how the binding of SH3 proteins to the polyproline region of WASP affects the localization of WASP to vesicles and the leading edge.

ACKNOWLEDGMENTS

We thank Joel Mulimba and Laura Leeper for excellent technical assistance. We also thank Drs. Alissa Weaver and Ann Richmond for useful discussions and critical reading of the manuscript. This work was supported, in part, by grants from National Institutes of Health (C.Y.C. and R.A.F.). C.Y.C. was partially supported by a grant from The Leukemia and Lymphoma Society (3965-01).

REFERENCES

Aldrich, R. A., Steinberg, A. G., and Campbell, D. C. (1954). Pedigree demonstrating a sex linked recessive condition characterized by draining ears, eczematoid dermatitis, and bloody diarrhea. Pediatrics *13*, 133–139.

Altman, L. C., Snyderman, R., and Blaese, R. M. (1974). Abnormalities of chemotactic lymphokine synthesis and mononuclear leukocyte chemotaxis in Wiskott-Aldrich syndrome. J. Clin. Invest. *54*, 486–493.

Asano, S., Mishima, M., and Nishida, E. (2001). Coronin forms a stable dimer through its C-terminal coiled coil region: an implicated role in its localization to cell periphery. Genes Cells *6*, 225–235.

Aubry, L., and Firtel, R. (1999). Integration of signaling networks that regulate *Dictyostelium* differentiation. Annu. Rev. Cell Dev. Biol. *15*, 469–4517.

Badolato, R., Sozzani, S., Malacarne, F., Bresciani, S., Fiorini, M., Borsatti, A., Albertini, A., Mantovani, A., Ugazio, A. G., and Notarangelo, L. D. (1998). Monocytes from Wiskott-Aldrich patients display reduced chemotaxis and lack of cell polarization in response to monocyte chemoattractant protein-1 and formyl-methionyl-leucyl-phenylalanine. J. Immunol. *161*, 1026–1033.

Badour, K., Zhang, J., and Siminovitch, K. A. (2003). The Wiskott-Aldrich syndrome protein: forging the link between actin and cell activation. Immunol. Rev. *192*, 98–112.

Bear, J. E., Rawls, J. F., and Saxe, C. L., 3rd. (1998). SCAR, a WASP-related protein, isolated as a suppressor of receptor defects in late *Dictyostelium* development. J. Cell Biol. *142*, 1325–1335.

Benesch, S., Lommel, S., Steffen, A., Stradal, T.E.B., Scaplehorn, N., Way, M., Wehland, J., and Rottner, K. (2002). Phosphatidylinositol 4,5-Biphosphate (PIP2)-induced vesicle movement depends on N-WASP and involves Nck, WIP, and Grb2. J. Biol. Chem. *277*, 37771–37776.

Blaauw, M., Linskens, M.H.K., and van Haastert, P.J.M. (2000). Efficient control of gene expression by a tetracycline-dependent transactivator in single *Dictyostelium discoideum* cells. Gene *252*, 71–82.

Borisy, G. G., and Svitkina, T. M. (2000). Actin machinery: pushing the envelope. Curr. Opin. Cell Biol. *12*, 104–112.

Bresnick, A. R., Warren, V., and Condeelis, J. (1990). Identification of a short sequence essential for actin binding by *Dictyostelium* ABP-120. J. Biol. Chem. *265*, 9236–9240.

Chung, C. Y., and Firtel, R. A. (1999). PAKa, a putative PAK family member, is required for cytokinesis and the regulation of the cytoskeleton in *Dictyostelium discoideum* cells during chemotaxis. J. Cell Biol. *147*, 559–575.

Chung, C. Y., Potikyan, G., and Firtel, R. A. (2001). Control of cell polarity and chemotaxis by Akt/PKB and PI3 kinase through the regulation of PAKa. Mol. Cell. *7*, 937–947.

Chung, C. Y., Reddy, T.B.K., Zhou, K. M., and Firtel, R. A. (1998). A novel, putative MEK kinase controls developmental timing and spatial patterning in *Dictyostelium* and is regulated by ubiquitin-mediated protein degradation. Genes Dev. *12*, 3564–3578.

Clow, P. A., and McNally, J. G. (1999). In vivo observations of myosin II dynamics support a role in rear retraction. Mol. Biol. Cell. *10*, 1309–1323.

Datta, S., and Firtel, R.A. (1987). Identification of the sequences controlling cyclic AMP regulation and cell-type specific expression of a prestalk-specific gene in *Dictyostelium discoideum*. Mol. Cell. Biol. *7*, 149–159.

de Hostos, E. L. (1999). The coronin family of actin-associated proteins. Trends Cell Biol. *9*, 345–350.

Deak, M., Casamayor, A., Currie, R. A., Downes, C. P., and Alessi, D. R. (1999). Characterisation of a plant 3-phosphoinositide-dependent protein kinase-1 homologue which contains a pleckstrin homology domain. FEBS Lett. *451*, 220–226.

Derry, J. M., Ochs, H. D., and Francke, U. (1994). Isolation of a novel gene mutated in Wiskott-Aldrich syndrome. Cell *78*: 635–644.

Devreotes, P., and Janetopoulos, C. (2003). Eukaryotic chemotaxis: distinctions between directional sensing and polarization. J. Biol. Chem. *278*, 20445–20448.

Downey, G. P. (1994). Mechanisms of leukocyte motility and chemotaxis. Curr. Opin. Immunol. *6*, 113–124.

Egelhoff, T. T., Naismith, T. V., and Brozovich, F. V. (1996). Myosin-based cortical tension in *Dictyostelium* resolved into heavy and light chain-regulated components. J. Muscle Res. Cell Motil. *17*, 269–274.

Firtel, R. A., and Chung, C. Y. (2000). The molecular genetics of chemotaxis: sensing and responding to chemoattractant gradients. BioEssays *22*, 603–615.

Firtel, R. A., and Meili, R. (2000). *Dictyostelium*: a model for regulated cell movement during morphogenesis. Curr. Opin. Genet. Dev. *10*, 421–427.

Funamoto, S., Meili, R., Lee, S., Parry, L., and Firtel, R. A. (2002). Spatial and temporal regulation of 3-phosphoinositides by PI3-kinase and PTEN mediates chemotaxis. Cell *109*, 611–623.

Funamoto, S., Milan, K., Meili, R., and Firtel, R. A. (2001). Role of PI3 kinase and a downstream PH domain-containing protein in controlling chemotaxis in *Dictyostelium.* J. Cell Biol. *153*, 795–809.

Futrelle, R. P., Traut, F. J., and McKee, W. G. (1982). Cell behavior in *Dictyostelium discoideum*: preaggregation response to localized cAMP pulses. J. Cell Biol. *92*, 807–821.

Gerisch, G., Albrecht, R., Heizer, C., Hodgkinson, S., and Maniak, M. (1995). Chemoattractant-controlled accumulation of coronin at the leading edge of *Dictyostelium* cells monitored using green fluorescent protein-coronin fusion protein. Curr. Biol. *5*, 1280–1285.

Hall, A. (1998). Rho GTPases and the actin cytoskeleton. Science *279*, 509–514.

Higgs, H. N., and Pollard, T. D. (2000). Activation by Cdc42 and PIP(2) of Wiskott-Aldrich syndrome protein (WASp) stimulates actin nucleation by Arp2/3 complex. J. Cell Biol. *150*, 1311–1320.

Ho, H.-Y.H., Rohatgi, R., Lebensohn, A., Ma, L., Li, J., Gygi, S. P., and Kirschner, M. (2004). Toca-1 mediates Cdc42-dependent actin nucleation by activating the N-WASP-WIP complex. Cell *118*, 203–216.

Hosaka, S., Suzuki, M., and Sato, H. (1979). Leucocyte-like motility of cancer cells, with reference to the mechanism of extravasation in metastasis. Gann *70*, 559–561.

Imai, K., Nonoyama, S., Miki, H., Morio, T., Fukami, K., Zhu, Q., Aruffo, A., Ochs, H.D., Yata, J., and Takenawa, T. (1999). The pleckstrin homology domain of the Wiskott-Aldrich syndrome protein is involved in the organization of actin cytoskeleton. Clin. Immunol. *92*, 128–137.

Insall, R. H., and Weiner, O. D. (2001). PIP3, PIP2, and cell movement—similar messages, different meanings? Dev. Cell *1*, 743–747.

Kim, A. S., Kakalis, L. T., Abdul-Manan, N., Liu, G. A., and Rosen, M. K. (2000). Autoinhibition and activation mechanisms of the Wiskott-Aldrich syndrome protein. Nature *404*, 151–158.

Lahrtz, F., Piali, L., Spanaus, K. S., Seebach, J., and Fontana, A. (1998). Chemokines and chemotaxis of leukocytes in infectious meningitis. J. Neuroimmunol. *85*, 33–43.

Li, R. (1997). Bee1, a yeast protein with homology to Wiscott-Aldrich syndrome protein, is critical for the assembly of cortical actin cytoskeleton. J. Cell Biol. *136*, 649–658.

Locker, J., Goldblatt, P. J., and Leighton, J. (1970). Ultrastructural features of invasion in chick embryo liver metastasis of *Yoshida* ascites hepatoma. Cancer Res. *30*, 1632–1644.

Machesky, L. M., and Insall, R. H. (1998). Scar1 and the related Wiskott-Aldrich syndrome protein, WASP, regulate the actin cytoskeleton through the Arp2/3 complex. Curr. Biol. *8*, 1347–1356.

Machesky, L. M., Mullins, R. D., Higgs, H. N., Kaiser, D. A., Blanchoin, L., May, R. C., Hall, M. E., and Pollard, T. D. (1999). Scar, a WASp-related protein, activates nucleation of actin filaments by the Arp2/3 complex. Proc. Natl. Acad. Sci. USA *96*, 3739–3744.

Marchand, J. B., Kaiser, D. A., Pollard, T. D., and Higgs, H. N. (2001). Interaction of WASP/Scar proteins with actin and vertebrate Arp2/3 complex. Nat. Cell Biol. *3*, 76–82.

Meili, R., Ellsworth, C., Lee, S., Reddy, T.B.K., Ma, H., and Firtel, R. A. (1999). Chemoattractant-mediated transient activation and membrane localization of Akt/PKB is required for efficient chemotaxis to cAMP in *Dictyostelium.* EMBO J. *18*, 2092–2105.

Merlot, S., and Firtel, R. A. (2003). Leading the way: directional sensing through phosphatidylinositol 3-kinase and other signaling pathways. J. Cell Sci. *116*, 3471–3478.

Miki, H., Miura, K., and Takenawa, T. (1996). N-WASP, a novel actin-depolymerizing protein, regulates the cortical cytoskeletal rearrangement in a PIP2-dependent manner downstream of tyrosine kinases. EMBO J. *15*, 5326–5335.

Ochs, H. D. (1998a). The Wiskott-Aldrich syndrome. Semin. Hematol. *35*, 332–345.

Ochs, H. D. (1998b). The Wiskott-Aldrich syndrome. Springer Semin. Immunopathol. *19*, 435–458.

Oikawa, T., Yamaguchi, H., Itoh, T., Kato, M., Ijuin, T., Yamazaki, D., Suetsugu, S., and Takenawa, T. (2004). PtdIns(3,4,5)P_3 binding is necessary for WAVE2-induced formation of lamellipodia. Nat. Cell Biol. *6*, 420–428.

Pang, K. M., Lee, E., and Knecht, D. A. (1998). Use of a fusion protein between GFP and an actin-binding domain to visualize transient filamentous-actin structures. Curr. Biol. *8*, 405–408.

Parent, C. A., Blacklock, B. J., Froehlich, W. M., Murphy, D. B., and Devreotes, P. N. (1998). G protein signaling events are activated at the leading edge of chemotactic cells. Cell *95*, 81–91.

Parent, C. A., and Devreotes, P. N. (1999). A cell's sense of direction. Science *284*, 765–770.

Prehoda, K. E., Scott, J. A., Mullins, R. D., and Lim, W. A. (2000). Integration of multiple signals through cooperative regulation of the N-WASP-Arp2/3 complex. Science *290*, 801–806.

Remold-O'Donnell, E., Cooley, J., Shcherbina, A., Hagemann, T. L., Kwan, S. P., Kenney, D. M., and Rosen, F. S. (1997). Variable expression of WASP in B cell lines of Wiskott-Aldrich syndrome patients. J. Immunol. *158*, 4021–4025.

Rickert, P., Weiner, O. D., Wang, F., Bourne, H. R., and Servant, G. (2000). Leukocytes navigate by compass: roles of PI3K[gamma] and its lipid products. Trends Cell Biol. *10*, 466–473.

Rodal, A. A., Manning, A. L., Goode, B. L., and Drubin, D. G. (2003). Negative regulation of yeast WASp by two SH3 domain-containing proteins. Curr. Biol. *13*, 1000–1008.

Rohatgi, R., Ho, H. Y., and Kirschner, M. W. (2000). Mechanism of N-WASP activation by CDC42 and phosphatidylinositol 4, 5-bisphosphate. J. Cell Biol. *150*, 1299–1310.

Rohatgi, R., Ma, L., Miki, H., Lopez, M., Kirchhausen, T., Takenawa, T., and Kirschner, M. W. (1999). The interaction between N-WASP and the Arp2/3 complex links Cdc42-dependent signals to actin assembly. Cell *97*, 221–231.

Sanchez-Madrid, F., and del Pozo, M. A. (1999). Leukocyte polarization in cell migration and immune interactions. EMBO J. *18*, 501–511.

Servant, G., Weiner, O. D., Herzmark, P., Balla, T., Sedat, J. W., and Bourne, H. R. (2000). Polarization of chemoattractant receptor signaling during neutrophil chemotaxis. Science *287*, 1037–1040.

Snapper, S. B. *et al.* (1998). Wiskott-Aldrich syndrome protein-deficient mice reveal a role for WASP in T but not B cell activation. Immunity *9*, 81–91.

Stites, J., Wessels, D., Uhl, A., Egelhoff, T., Shutt, D., and Soll, D. R. (1998). Phosphorylation of the *Dictyostelium* myosin II heavy chain is necessary for maintaining cellular polarity and suppressing turning during chemotaxis. Cell Motil. Cytoskeleton *39*, 31–51.

Symons, M., Derry, J. M., Karlak, B., Jiang, S., Lemahieu, V., McCormick, F., Francke, U., and Abo, A. (1996). Wiskott-Aldrich syndrome protein, a novel effector for the GTPase CDC42Hs, is implicated in actin polymerization. Cell *84*, 723–734.

Thrasher, A. J., Burns, S., Lorenzi, R., and Jones, G. E. (2000). The Wiskott-Aldrich syndrome: disordered actin dynamics in haematopoietic cells. Immunol. Rev. *178*, 118–128.

Wang, F., Herzmark, P., Weiner, O. D., Srinivasan, S., Servant, G., and Bourne, H. R. (2002). Lipid products of PI(3)Ks maintain persistent cell polarity and directed motility in neutrophils. Nat. Cell Biol. *4*, 513–518.

Weijer, C.J. (1999). Morphogenetic cell movement in *Dictyostelium*. Semin. Cell Dev. Biol. *10*, 609–619.

Westerberg, L., Greicius, G., Snapper, S. B., Aspenstrom, P., and Severinson, E. (2001). Cdc42, Rac1, and the Wiskott-Aldrich syndrome protein are involved in the cytoskeletal regulation of B lymphocytes. Blood *98*, 1086–1094.

Westphal, M., Jungbluth, A., Heidecker, M., Muhlbauer, B., Heizer, C., Schwartz, J. M., Marriott, G., and Gerisch, G. (1997). Microfilament dynamics during cell movement and chemotaxis monitored using a GFP-actin fusion protein. Curr. Biol. *7*, 176–183.

Yarar, D., D'Alessio, J. A., Jeng, R. L., and Welch, M. D. (2002). Motility determinants in WASP family proteins. Mol. Biol. Cell *13*, 4045–4059.

Zalevsky, J., Lempert, L., Kranitz, H., and Mullins, R. D. (2001). Different WASP family proteins stimulate different Arp2/3 complex-dependent actin-nucleating activities. Curr. Biol. *11*, 1903–1913.

Zallen, J. A., Cohen, Y., Hudson, A. M., Cooley, L., Wieschaus, E., and Schejter, E. D. (2002). SCAR is a primary regulator of Arp2/3-dependent morphological events in *Drosophila*. J. Cell Biol. *156*, 689–701.

Zicha, D., Allen, W. E., Brickell, P. M., Kinnon, C., Dunn, G. A., Jones, G. E., and Thrasher, A. J. (1998). Chemotaxis of macrophages is abolished in the Wiskott-Aldrich syndrome. Br. J. Haematol. *101*, 659–665.

Zigmond, S. H. (2000). How WASP regulates actin polymerization. J. Cell Biol. *150*, F117–F120.

Zigmond, S. H., Joyce, M., Borleis, J., Bokoch, G. M., and Devreotes, P. N. (1997). Regulation of actin polymerization in cell-free systems by GTPgammaS and Cdc42. J. Cell Biol. *138*, 363–374.